

1 **SUPPLEMENTAL INFORMATION**
2
3
4
5

6 **TENM4 is an essential transduction component for touch**
7
8

9 Corresponding author: Gary R. Lewin, glewin@mdc-berlin.de
10
11
12

13 **The file includes:**

14 Method details

15 Figures S1 to S11

16 Tables S1 to S2

17 References

18

19

20

21

22

23 **Methods details**24 **Animals**

25 All experiments were approved by the Berlin Animal Ethics Committees (Landesamt für Gesundheit und
26 Soziales) and carried out in accordance with European animal welfare law. Wild-type (C57BL/6N) adult
27 (8-30 weeks) mice of both sexes were used. Mice were housed in groups of 5 with food, water and
28 enrichment available ad libitum.

29 The *Tenm4*^{KI/+} mouse line was generated by the Ingenious Targeting Laboratory (Ronkonkoma, NY) using
30 homologous recombination in mouse ES cells. Targeted iTL IN2 (C57BL/6) embryonic stem cells were
31 microinjected into Balb/c blastocysts. Resulting chimeras with a high percentage black coat color were
32 mated to C57BL/6 FLP mice to generate Somatic Neo Deleted mice. This involved the replacement of the
33 amino acids HLYTQSL (exon 27) with the PreScission Protease target sequence LEVLFQG, as illustrated
34 in Figure S2. After the removal of the Neo cassette, a single FRT site of 78 bp is retained and subsequently
35 utilized for the selection process and genotyping. The genotyping strategy utilized was as follows: Forward
36 primer: 5'- GGGAAATGGGATGGTGGGAA -3', reverse primer: 5'- ACCCACGTGGAGTTGTTCTTC
37 -3'. The expected band for WT is 231 bp, while for *Tenm4*^{KI/+}, two bands are observed at 231 and 309 bp.
38 *Frem2*^{f/f} and *Tenm4*^{f/f} mouse lines were generated at Shanghai Model Organisms Center using the
39 CRISPR/Cas9 strategy. *Frem2*^{f/f} and *Tenm4*^{f/f} mice, carrying LoxP sites flanking exon 12 and exon 7,
40 respectively, were generated using the following gRNAs *Frem2*^{f/f}-gRNA1 (5'-
41 ACAAGACTAGCTCTGGTCTGGG -3'), *Frem2*^{f/f}-gRNA2 (5'-
42 TACAGAGATAACAGTGGGGTGG -3'), *Tenm4*^{f/f}-gRNA1 (5'-
43 AGAGCCCAGTCTCTCACCACTGG -3') and *Tenm4*^{f/f}-gRNA2 (5'-
44 GCACTGAACCTCAGCCCTGGTGG -3'). The *Frem2*^{f/f} genotyping strategy utilized was as follows:
45 forward primer (5'- AGTCGGGTTCTTCTTCCACAA -3'), reverse primer (5'-
46 CCCAAAAGGTCACATGCTAATCTAT -3'). The expected band for WT is 197 bp, while for *Frem2*^{f/f},
47 a band with 263 bp. The *Tenm4*^{f/f} genotyping strategy utilized was as follows: forward primer (5'-
48 TGAACCATGCATCCCTCACC -3'), reverse primer (5'- AAACTCCCACCCCACTGAAC -3'). The
49 expected band for WT is 313 bp, while for *Tenm4*^{f/f}, a band with 379 bp. Animals of various genotypes
50 were randomly selected for experiments based on their availability.

51 *Pv-Cre;Tenm4*^{f/f} mice were generated by crossing *Pv*^{Cre} (B6;129P2-*Pvalb*^{tm1(cre)Arbr}/J;
52 RRID:IMSR_JAX:008069) mice and *Tenm4*^{f/f} mice. *PV*^{cre}; *Rx3*^{fpo}; Ai65D mice were generated by crossing
53 *PV*^{cre} and *Rx3*^{fpo} lines with the Ai65D reporter allele to create a triple transgenic line that selectively labels
54 proprioceptive sensory neurons.¹⁻³ Muscle spindles and Golgi tendon organs (GTOs) are unique in that
55 they are the only cells in the mouse body that co-express parvalbumin (PV) and the transcription factor
56 RUNX3 (Rx3). This molecular intersection provides a highly specific genetic entry point for targeting
57 proprioceptors.³ In the *PV*^{cre}; *Rx3*^{fpo}; Ai65D line, cre- and flp-dependent recombination at the Ai65D locus

58 induces robust expression of tdTomato exclusively in proprioceptive DRG neurons and their peripheral
59 and central projections. This strategy enables the precise anatomical visualization of proprioceptive
60 terminals within muscle and provides a reliable reporter for experiments requiring the identification of
61 spindle and tendon organ afferents.

62

63 **AAV transduction**

64 *pAAV-Syn-Cre-p2A-EGFP* (4.91×10^{12} vg/ml) and *pAAV-hSyn-NLS-GFP-P2A* (4.98×10^{12} vg/ml) were
65 manufactured in the Charité Viral Core facility (Berlin, Germany). *Frem2*^{CKO} 765 and *Tenm4*^{CKO} were
66 generated by retroorbital injection of Adeno-associated virus (*pAAV-Syn-Cre-p2A-EGFP*) in *Frem2*^{f/f} and
67 *Tenm4*^{f/f}, respectively, to induce Cre/GFP recombinase expression in DRG neurons. Subsequently, DNA
68 between the LoxP sites will be excised, leading to a frameshift mutation and the production of a truncated
69 protein as illustrated in Figure S2. Control mice were generated by similar injections of *pAAV-hSyn-NLS-*
70 *GFP-P2A* that induce GFP expression in DRG neurons. Afterwards the animals were returned to their
71 home cage for at least three weeks to achieve an adequate recombination and subsequently tested in
72 electrophysiological and behavioral assays.

73

74 **Tamoxifen injections**

75 Tamoxifen-induced activation of Cre recombinase under the Advillin promoter in sensory neurons was
76 used as a second inducible approach to delete *Tenm4* using the AdvillinCreERT2 transgenic mice
77 (*Tenm4*^{f/f}; *Avil*^{CreERT2/WT}). Briefly, *Tenm4*^{f/f}; *Avil*^{CreERT2/WT} mice were injected intraperitoneally with corn
78 oil (control animals) or Tamoxifen (15mg/ml) solubilized in corn oil (Sigma) for 5 consecutive days. Prior
79 to injection, each mouse was weighed to ensure the administration of a uniform tamoxifen dose (150
80 mg/kg). Behavioral assays were performed 21 days after vehicle or tamoxifen injections.

81

82 **PreScission injections and ex vivo cleavage assay**

83 Adult mice (8-30 weeks old) were anesthetized using a 5% isoflurane-air mixture in a transparent box, with
84 anesthesia maintenance via a 2.5% isoflurane-air mixture through a plastic tube. After achieving slow,
85 steady breathing, a hind paw pinch test assessed pain reflexes. Subsequently, mice received a 10 μ L
86 injection of saline NaCl solution (control group) or a 20% diluted PreScission protease in saline NaCl
87 solution (v/v) 10 U/ μ L, Cytiva, Lot: 18043250). The injection was directed into the intraplanar surface of
88 glabrous skin or the top of the hairy skin of the hind paw. The mice were then used for for
89 immunohistochemistry, electrophysiological, or behavioral experiments.

90 For *ex vivo* PreScission protein cleavage assay, *Tenm4*^{KI/+} and WT mice were administered injections of
91 20% PreScission protease (2-10 U/ μ L, Cytiva, Lot: 18043250) diluted in NaCl (v/v) in the glabrous skin
92 of hind paws. Tissues were collected one-hour post-injection for protein extraction. Frozen tissues (-80°C)

93 were powdered using a mortar and added to lysis buffer (RIPA) containing 50 mM Tris pH 7.5, 150 mM
94 NaCl, 0.1% SDS, 1.0% NP-40, 0.5% deoxycholate, and a protease inhibitor cocktail tablet. Sonication
95 (magnitude 3) with 10 seconds on and 50 seconds off was applied three times to each sample. The lysate
96 was centrifuged at 13,200xg for 30 minutes. Samples corresponding to 1/100 of the input were resolved
97 by SDS-PAGE. Analysis was conducted by Western blotting using a polyclonal sheep-raised antibody
98 against TENM4 (dilution 1:500), followed by an HRP-conjugated goat anti-sheep IgG (R&D Lot:
99 1522051, dilution 1:10,000). Blots were developed using the SuperSignal™ West Dura ECL Kit (Thermo
100 Scientific) and imaged using a Bio-Rad ChemiDoc™ MP imaging system.

101

102 **Plasmids and cloning**

103 Teneurins 1-4 and Elkin1 were independently cloned into modified plasmids, incorporating the BsmBI
104 restriction site as detailed in the tripartite-GFP method section. This involved using specific primers for
105 each construct: TENM1 (1-526): forward primer (5'-cacgtctactccatggagcaaacagactgcaaa -3'), reverse
106 primer (5'-cacgtctcaattcaattgttagttgcacaaat-3'), TENM2 (1-571): forward primer (5'-
107 cacgtctcaattcaattgttagttgcacaaat -3'), reverse primer (5' ggatctgaattctaataagacaacagtgtgaaggag -
108 3'), TENM3 (1-513): forward primer (5'-cacgtctactccatggatgtgaaggaacgcag -3'), reverse primer (5'-
109 cacgtctcaattctataacgatcggttaaaggagac -3'), TENM4 (1-561): forward primer (5'-
110 cacgtctcaattccatggagccagaccactcg -3'), reverse primer (5'- cacgtctcaattccatggatgtgaaggacgg -3'), and
111 Elkin1 (full length): forward primer (5'- cacgtctcacaccatggcggtggctgc -3'), reverse primer (5'-
112 cacgtctcatccctccatttgaccttcaaagtg 3') (Clontech). The full-length Tenm4 cDNA, sourced from
113 VectorBuilder.inc (Mouse MGC Verified FL clone, ID: NM_011858.4, VB221104-1135), containing a
114 modified C-terminus ALFA tag. Additionally, the full-length PIEZO2 cDNA with an mScarlet red
115 fluorescent 820 protein tag plasmid was obtained as a gift from Professor Stefan Lechner at UKE Hamburg.
116 Furthermore, the recently-published full-length ELKIN1 pRK8-eGFP,⁴ was adapted to incorporate
117 mScarlet at the N-terminus using specific primers forward primer (5'-
118 ctatcgattgaattaagcttatggtagcaagggcgag -3'), reverse primer (5'-
119 caccgccatggggatccctgtacagctcgccatgcc -3') (Clontech).

120

121 **Cell line culture**

122 HEK293T cells were cultured in DMEM-Glutamax (Gibco, ThermoFisher Scientific) supplemented with
123 10% fetal bovine serum (FBS, PAN Biotech GmbH) and 1% penicillin and streptomycin (P/S, Sigma-
124 Aldrich). N2a cells were cultured in DMEM-Glutamax (Gibco, ThermoFisher Scientific) supplemented
125 with 45% Opti-MEM (Gibco, ThermoFisher Scientific), 10% FBS, and 1% penicillin and streptomycin
126 (P/S, Sigma-Aldrich). For downstream analyses, HEK293T and N2a cells were transiently transfected by
127 plating them on glass coverslips coated with poly-L-lysine and laminin at various cell densities and

128 maintained overnight in a 37°C, 5% CO2 incubator. Transfections were carried out using 4µL FuGene HD
129 per 50µL of Opti-MEM with 1µg of cDNA, following the manufacturer's instructions. Subsequent analyses
130 were performed 48 hours post-transfection, and data were derived from a minimum of 3 independent
131 transfections.

132

133 **siRNA transfection**

134 2 hours after plating the N2a cell in glass bottomed dishes coated with PLL and laminin, siRNA transfection
135 was carried out using DharmaFECT (Horizon) reagents according to the manufacturers' guidelines. Briefly,
136 siRNAs were mixed with serum and antibiotics free plating medium in a tube (total volume of 100 µl per
137 dish), and 4.5 µl of DharmaFECT 1 transfection reagent was mixed with serum and antibiotics free medium
138 (total volume of 100 µl) in another tube. Each tube was incubated separately for 5 min at RT, then mixed
139 together and incubated for a further 20 min. 800 µl of antibiotics free complete medium was added to this
140 mixture and added to the cells. Experimental dishes were transfected with a final concentration of 50 nM
141 ON-TARGETplus SMARTpool mTmem87a and 50 nM of siGLO green transfection indicator and control
142 dishes were transfected with 50 nM of ON-TARGETplus Non-targeting Pool and 50 nM of siGLO green
143 transfection indicator. Cells were transfected with mTenm4 using FuGene HD 24 hours after siRNA
144 transfection and patched 48 hours post-siRNA treatment. n=3.

145

146 **Immunocytochemistry**

147 Cells were fixed in 4% paraformaldehyde in PBS for 10 minutes at room temperature, followed by three
148 washes with PBS. Subsequently, cells were blocked for 1 hour with 10% horse serum in PBS, either in the
149 presence or absence of 0.1% (v/v) Triton X-100 for staining intracellular or extracellular epitopes,
150 respectively. Following blocking, cells were incubated overnight at 4°C with primary antibodies,
151 appropriately diluted in either 3% horse serum in PBS or 3% horse serum in 0.1% (v/v) Triton X-100/PBS,
152 depending on the location of the epitope, for epifluorescence staining or cellular staining, respectively.
153 Primary antibodies included polyclonal sheep anti-TENM4 antibody at a dilution of 1:500 (R&D Systems
154 (TENM4-N), Catalog #: AF6320), our own polyclonal rabbit anti-TENM4 antibody at a dilution of 1:1000
155 (TENM4-C) (Eurogentec), and FluoTag®-X2 anti-ALFA at a dilution of 1:500 (NanoTag, N1502-
156 Ab635P-L). When FluoTag®-X2 anti-ALFA was employed for Alfa-tagged protein detection, the
157 incubation time was reduced to 1.5 hours at room temperature. Following three washes with PBS, cells
158 were incubated for 1.5 hours at room temperature with species-specific conjugated secondary antibodies
159 diluted at 1:500 in PBS: Donkey anti-Sheep IgG (H+L) Cross-Adsorbed Secondary Antibody, Alexa
160 Fluor™ 568 (Invitrogen, Catalog # A-21099), and goat anti-Rabbit IgG (H+L) Cross-Adsorbed Secondary
161 Antibody, Alexa Fluor™ 555 (Invitrogen, Catalog # A-21428). This step was omitted when using
162 FluoTag®-X2 anti-ALFA. After three washes in PBS, cells were stained with DAPI diluted 1:1000 in PBS

163 for 10 minutes at room temperature, followed by three additional washes in PBS, and finally, mounting
164 with Dako (Agilent, S3023).

165

166 **Multiplex fluorescent *in situ* hybridization**

167 *Tenm4*, *Kcnq4*, *Elkin1* and *Piezo2* mRNA levels were assessed in DRGs from WT (n = 4) mice using
168 RNAscope Multiplex Fluorescent Kit v2 (a fluorescent *in situ* hybridization technology). Briefly, the 12 μ m
169 DRG sections were immersed in PBS for 15 minutes and dehydrated in a series of 50 %, 70 %, 100 %
170 ethanol for 5 minutes each. Afterwards, sections were treated with a hydrogen peroxide solution for 15
171 minutes at room temperature to block endogenous peroxidase activity followed by another wash with 100%
172 ethanol for 5 minutes. Next, Protease plus was applied for 30 minutes at RT. After three washes with PBS,
173 probes were applied, and hybridization was carried out in a humified oven at 40°C for 2h. Following
174 hybridization, amplification was performed using Amp1, Amp2, and Amp3 each for 30 minutes at 40°C.
175 For detection, each section was treated sequentially with channel specific HRP (HRP-C1, HRP-C1, HRP-
176 C3) for 15 minutes, followed by TSA-mediated fluorophore binding for 30 minutes and final HRP blocking
177 for 15 minutes (all steps at 40°C). The following probes were used: *Tenm4*- Mm-*Tenm4* (C1 #555491),
178 *Kcnq4*- Mm-*Kcnq4* (C2 #472271), *Piezo2* - Mm-*Piezo2*-E43-E45 15 (C1 #439971) and *Elkin1* - Mm-
179 *Tmem87a* (C3 #868581). The fluorophores applied to detect the signal from the probes were Opal 690
180 Reagent (1:750; Akoya Biosciences, #FP1497001KT) or Opal 570 Reagent (1:750; Akoya Biosciences,
181 #FP1488001KT). Slides were rinsed with PBS-tween, followed by a 1-hour incubation at room temperature
182 in an antibody diluent solution. Following this, they were treated for antibody immunostaining according
183 to procedures outlined below. Lastly, the slides were exposed to RNAscope DAPI during the final
184 incubation. Images were obtained using Airyscan fluorescence microscope (Axio, Zeiss). Exposure levels
185 were kept constant for each slide and the same contrast enhancements were made to all slides. In the
186 quantification experiments, over 700 neurons were counted in each group, with a representation of 2 male
187 and 3 female mice in each group.

188

189 **Generation of anti TENM4 antibody (Anti-TENM4-C)**

190 The antigen used for the generation of this polyclonal antibody consisted of most of the extracellular
191 domain of murine TENM4 (UniProt ID Q3UHK6), including the large YD shell. The expression construct
192 for the production of the antigen was synthesized by VectorBuilder GmbH (pRP[Exp]-CMV) and
193 comprised amino acids 921 to 2771, resulting in secretion,⁵ (μ phosphatase secretion leader sequence
194 MGILPSPGMPALLSLVSLLSVLLMGCVVA*ETG) of a C-terminal His6-tagged protein. The protein was
195 produced in ExpiCHO-STM cells (Thermo Fisher Scientific) at 31°C and 8% CO₂ using BalanCD
196 transfectory CHO medium (FUJIFILM Irvine Scientific) supplemented with 4 mM GlutaMAX (Thermo
197 Fisher Scientific). Cells were transiently transfected using PEI MAX (Polysciences) and supplemented

198 with 6 g/L glucose (Sigma) three days after transfection. Cell culture supernatant was collected six days
199 after transfection, filtered through 0.22 μ m filters, and supplemented with 0.5 M NaCl, 5 mM imidazole,
200 and 25 mM sodium phosphate buffer pH 7.8. The protein was captured from the supernatant by affinity
201 chromatography using cComplete™ His-Tag Purification Resin (Roche), equilibrated with 50 mM sodium
202 phosphate pH 7.8, 0.5 M NaCl, and 5 mM imidazole. The bound protein was first washed with 50 mM sodium
203 phosphate pH 7.8, 0.5 M NaCl, followed by a buffer containing 10 mM imidazole to remove
204 contaminating proteins. The protein was eluted with the same buffer containing 0.25 M imidazole. The
205 protein was further purified by gel filtration on a 16/60 HiPrep Sephacryl S-400 HR column (Cytiva)
206 equilibrated with PBS buffer pH 7.4 and 0.2 M NaCl. The purified protein was concentrated to about 3
207 mg/mL, sterile filtered, flash-frozen in small aliquots with liquid nitrogen and stored at -70°C until further
208 use.

209 The purified antigen was then used by Eurogentec for immunization of rabbits. Two animals were injected
210 4 times with 100 μ g of antigen. The final bleed was collected 28 days after the first injection and
211 subsequently concentrated using affinity purification.

212

213 **Immunohistochemistry**

214 Mice were euthanized by cervical dislocation, and tissues including hairy and glabrous skin, sciatic nerves,
215 and DRGs, were collected. The hairy skins were shaved, and the hypodermis, ligaments, and attached
216 muscle tissue were removed from the skin samples. Subsequently, skin samples were stretched out using
217 insect pins and fixed in 4% paraformaldehyde (PFA) for a duration of 4 hours then post-fixed at 4 °C for
218 24 h in 20% dimethylsulfoxide and 80% methanol, while sciatic nerve and DRG samples were fixed in 4%
219 PFA for a duration of 2 hours. L2–L5 DRG and sciatic nerves were dissected and postfixed in PFA for 1
220 hour. Samples underwent cryoprotection with an overnight incubation in 30% (w/v) sucrose solution in
221 5% PBS at 4 °C, followed by embedding in optimal cutting temperature compound (OCT compound;
222 Thermo Fisher Scientific).

223 *PV^{cre};Rx3^{flop};Ai65D* mice were deeply anaesthetized and transcardially perfused with 1xPBS, followed by
224 4% PFA in 1xPBS. The *tibialis anterior* muscles were then dissected and post-fixed in 4% PFA at 4 °C
225 overnight, and subsequently cryoprotected in 30% sucrose in 1xPBS until they sank. The muscles were
226 then embedded in OCT.

227 Abdominal human skin samples were obtained from patients that underwent plastic surgery (written
228 consent obtained, ethics approval from Charité University Hospital EA1/356/21). Following surgical
229 removal, excessive subcutaneous fat tissue was removed and skin sheets were either directly used or stored
230 at -20 °C until further usage.

231 OCT-embedded samples were snap-frozen on dry ice and stored at -80 °C. Sciatic nerve- and DRGs-
232 embedded tissues were sectioned at 12 μ m using a Leica Cryostat (CM3000; Nussloch), mounted on

233 Superfrost-Plus microscope slides (Thermo Fisher Scientific) and stored at -80 °C until staining. Skin-
234 embedded tissues were sectioned at 60 µm and stored in freezing solution (30% (v:v) glycerol, 30%
235 ethylene glycol, and 40% PBS). During staining, slides and free-floating skin sections were washed with
236 PBS-tween and blocked in antibody diluent solution containing 0.2% (v/v) Triton X-100, 5% (v/v) horse
237 serum, and 1% (v/v) bovine serum albumin in PBS for 1 hour at room temperature. Subsequently, slides
238 underwent a 12-hour incubation, while skin samples were incubated for 72 hours at 4 °C with primary
239 antibodies. OCT-embedded muscle tissue was sectioned at 50 µm using a cryostat (Leica CM3050 S;
240 Nussloch), mounted on Superfrost-Plus microscope slides (Thermo Fisher Scientific) and stored at -80 °C
241 until staining. The following primary antibodies were used: anti-TENM4 (host: sheep, AF6320 and
242 ab215052, 1:500), anti-S100 (host: rabbit, 15146-1-AP, 1:1000), anti-NF200 (host: chicken, AB72996,
243 1:1000), anti-CK20 (host: guinea pig, BP5080, 1:500), anti-CGRP (host: rabbit, 24112, 1:500), anti-TH
244 (host: sheep, AB1542, 1:1000), anti-TRKC (host: goat, AF1404, 1:1000), anti-Frem2 (host: rabbit, sc-
245 98471, 1:400), anti-Slit1 (host: rabbit, ab10984, 1:400), anti-Scribble (host: rabbit, ab154067, 1:400), anti-
246 Pcsk5 (host: rabbit, TA332044, 1:400), anti-Tecta (host: mouse, ABNOH00007007-A01, 1:100). Slides
247 and free-floating skin sections were then washed three times using PBS-tween and incubated with the
248 following species-specific conjugated secondary antibodies at 1:500 dilution: Alexa Fluor 488 anti-rabbit
249 (A21206), Alexa Fluor 568 anti-sheep (A21099), Alexa Fluor 568 anti-chicken (A11041), Alexa Fluor 555
250 anti-goat (A21432), Alexa Fluor 568 anti-guinea pig (106-165-003), or Isolectin GS B4 conjugated to Alexa
251 594 (121413, Thermo Fisher) overnight at 4 °C. The secondary antibody was washed three times in PBS
252 tween. DRG and sciatic nerve slides were then mounted with Dako (Agilent, S3023), muscle slides were
253 mounted with Mowiol Mounting Medium (Roth, 0713.2), while skin samples were processed for tissue
254 clearing using 2,2'-thiodiethanol (TDE, Sigma-Aldrich). Skin sections were then placed in increasing
255 concentrations of TDE every 2 h, from 10% to 25%, 50% and 97%, in which samples were stored and
256 mounted on to slides and cover slipped. Slides and free-floating skin sections were imaged with Airyscan
257 fluorescence microscope (Axio, Zeiss). Muscle slides were imaged with a confocal laser scanning
258 microscope (Zeiss LSM 800). Exposure levels were kept constant for each slide and the same contrast
259 enhancements were made to all slides. Negative controls without the primary antibody showed no staining
260 with either secondary. In the quantification experiments, over 700 neurons were counted in each group,
261 with a representation of 2 male and 3 female mice in each group.

262

263 **DRG neuron culture**

264 Lumbar DRGs (L1-L6) were collected from mice into plating medium (DMEM-F12, Gibco, ThermoFisher
265 Scientific) supplemented with 10% fetal horse serum (FHS, Life Technologies) and 1% penicillin and
266 streptomycin (P/S, Sigma-Aldrich). A single-cell suspension was obtained by enzymatic digestion, first in
267 1.25% Collagenase IV (1 mg/ml, Sigma-Aldrich) for 1 hour at 37°C and then in 2.5% Trypsin (Sigma-

268 Aldrich) for 15 minutes at 37°C, followed by mechanical trituration with a P1000 pipette tip and
269 purification on a 15% fraction V BSA column. Subsequently, neurons were plated on glass-bottomed
270 dishes coated with poly-L-lysine and laminin for indentation assays or immunostaining. The cultured
271 neurons were incubated in a standard incubator (37°C and 5% CO₂). Electrophysiological experiments
272 involving indentation were conducted 18-24 hours after plating, while immunostaining experiments were
273 performed 48 hours after plating. For the MA-current analysis of *Tenm4*^{fl/fl} animals, n = 4 mice underwent
274 AAV-GFP injection (control), and n = 5 mice underwent AAV-Cre injection. For the MA-current analysis
275 of the effects of PreScission on WT and *TENM4*^{KI/+} mice, n = 5 WT, and n = 4 *TENM4*^{KI/+} mice were
276 utilized. Sample sizes were determined based on previous studies with similar effect sizes.

277

278 **Real-time PCR**

279 Total RNA was extracted from the skin, DRG, and sciatic nerve of WT mice using the ReliaPrep™ RNA
280 Miniprep Systems and retro-transcribed into cDNA using the GoScript™ Reverse Transcriptase kit,
281 according to the manufacturer's instructions. The expression of TENM4 was evaluated using SYBR Green
282 Real-Time PCR (Thermo Fisher Scientific™). The PCR mix contained 2µl of a 1:10 diluted cDNA
283 template; 5µl of 2x SYBR® Green Master Mix (BioRad); 0.3µl of a 10µM forward primer; 0.3µl of a
284 10µM reverse primer; 0.5µl of DMSO; 1.9µl of H₂O, in a total volume of 10µl per sample. The primers
285 used were the forward primer (5' – cccatcagcaactctcaggac -3') and the reverse primer (5'-
286 ccccgaggatagacttgct -3'). Standard reactions were carried out using a CFX Connect RealTime PCR
287 Detection System. Technical triplicates were included in each experiment. Standard curves obtained with
288 the amplification of standard plasmids at increasing known concentrations were used to quantify TENM4
289 expression in different tissues.

290

291 **Whole-cell patch clamp**

292 Neurons or transfected N2a^{*Piezo1*−/−} cells^{6,7} were immersed in an extracellular solution composed of (in mM):
293 140 NaCl, 4 KCl, 2 CaCl₂, 1 MgCl₂, 4 Glucose and 10 HEPES, pH adjusted to 7.4 with NaOH. For the
294 MA-current analysis of the effects of PreScission on WT and *Tenm4*^{KI/+} mice, neurons were immersed in
295 the identical extracellular solution, supplemented with PreScission protease at a ratio of 2:1000 (v/v), 30
296 minutes prior to recordings. Patch pipettes (3-6 MΩ resistance) were fashioned from heat-polished
297 borosilicate glass (Harvard apparatus, 1.17 mm x 0.87 mm) and filled with an intracellular solution
298 containing (in mM): 110 KCl, 10 NaCl, 1 MgCl₂, 1 EGTA, and 10 HEPES, with pH adjusted to 7.3 using
299 KOH. Current-clamp experiments involved injecting steps of current in 50 pA increments from 0-950 pA
300 to categorize sensory neurons into mechano- (large neurons) and nociceptors (small/medium neurons).
301 Currents from neurons or transfected N2a^{*Piezo1*−/−} cells were evoked using pillar deflection at a holding
302 potential of -60 mV. Recordings were acquired with an EPC-10 amplifier with Patchmaster software

303 (HEKA, Elektronik GmbH, Germany). For indentation experiments, neuronal cell membrane indentation
304 in the range of 1 – 9 μm was achieved using a heat-polished borosilicate glass pipette (mechanical
305 stimulator) manipulated by a MM3A micromanipulator. Bright field images were captured with a 40X
306 objective and a CoolSnapEZ camera (Photometrics, Tucson, AZ) on a Zeiss 200 inverted microscope for
307 the analysis of neuronal diameter. Currents and biophysical parameters were analyzed using FitMaster
308 (HEKA, Elektronik GmbH, Germany).

309

310 **Pillar arrays**

311 Pillar arrays were prepared as described previously.^{4,6,8,9} Briefly, salinized negative masters were used as
312 templates. Negative masters were covered with degassed polydimethylsiloxane (PDMS, sylgard 184
313 silicone elastomer kit, Dow Corning Corporation) mixed with a curing agent at 10:1 ratio. After 30 min,
314 glass coverslips were placed on the top of the negative masters containing 35 μm PDMS mix and baked at
315 110°C for 60 min. The pillar arrays were peeled away from the master. The resulting dimensions of single
316 pilus within the array was radius= 1.79 μm ; length= 5.87 μm . While the elasticity was 2.1 MPa and the
317 spring constant was 251 pN-nm as previously reported.^{4,6,8,9} The pillar arrays were plasma cleaned (Deiner
318 Electronic GmbH, Germany) and coated with PLL, subsequently N2a^{Piezol-/-} cells were cultured and were
319 prepared as previously described. 24 hours after cells adherent on pillar, cells were transfected with either
320 pRP TENM4-ALFA or pRK8 eGFP. After 24 hours of transfection, all cells were stained with FluoTag®-
321 X2 anti-ALFA, as described earlier without fixation and Triton X-100. GFP cells or live-staining positive
322 cells from respective cultures were selected for subsequent experiment.

323 To create quantitative data an individual pilus subjacent to the cell membrane was deflected using a heat-
324 polished borosilicate glass pipette (approx. 2 mm in diameter) driven by a MM3A micromanipulator
325 (Kleindiek Nanotechnik, Germany) as previously described in.^{4,6,8,9} Deflection stimuli were applied to a
326 single pilus in the range of 1-1000 nm and cells were monitored using whole-cell patch-clamp. A bright-
327 field image (Zeiss Axio Observer A1 inverted microscope) was taken before and during pillar deflection
328 stimuli using a CoolSnapEZ camera (Photometrics, Tucson, AZ) and 40x objective. The pillar deflection
329 was calculated by comparing the light intensity of the center of each pilus before and after the stimuli with
330 a 2D-Gaussian fit (Igor Software, WaveMetrics, USA). Stimuli larger than 1000 nm were excluded.

331

332 **Ex vivo skin nerve**

333 Ex vivo skin nerve electrophysiology was performed on cutaneous sensory fibers of the tibial and
334 saphenous nerves, following a previously established method.¹⁰ Briefly, mice were euthanized by cervical
335 dislocation, and the hair on the limb was shaved off. The hairy skin from the hind paw, along with the
336 saphenous nerve up to the hip, was then dissected. The innervated hairy skin was placed in a bath chamber
337 continuously perfused with warm (32°C) carbonated (95% O₂, 5% CO₂) interstitial fluid (SIF buffer): 123

338 mM NaCl, 3.5 mM KCl, 0.7 mM MgSO₄, 1.7 mM NaH₂PO₄, 2.0 mM CaCl₂, 9.5 mM sodium gluconate,
339 5.5 mM glucose, 7.5 mM sucrose, and 10 mM HEPES (pH 7.4). The skin was stretched and fixed "inside-
340 out" using insect needles, allowing stimulation of the inner part of the skin with stimulator probes. For the
341 glabrous skin, the tips of the toes were removed, and the skin was peeled back up to the ankle. The ankle
342 was circumferentially cut, and the sciatic nerve was freed at hip level. The foot with the tibial nerve was
343 placed in the organ bath chamber with superfused 30°C SIF buffer. Remaining muscle tissue, bones, and
344 tendons were removed, and the skin was fixed in the "outside-out" configuration. The nerve was guided
345 through a small opening to an adjacent chamber filled with mineral oil, where fine filaments were teased
346 from the nerve and placed on a silver wire recording electrode.

347 Mechanically sensitive units were initially identified using blunt stimuli applied with a glass rod.
348 Classification of mechanoreceptors was based on spike pattern and sensitivity to stimulus velocity, as
349 described previously.^{10–12} Raw electrophysiological data were recorded using a Powerlab 4/30 system and
350 Labchart 8 software, with the spike-histogram extension supported by an oscilloscope for visual
351 identification and subsequent analysis. All mechanical responses analyzed were adjusted for the latency
352 delay between the electrical stimulus and the arrival of the action potential at the electrode.

353 Conduction velocity (CV) was measured using the formula CV = distance/time delay, where CVs > 10 m/s
354 were classified as rapidly adapting mechanoreceptors (RAMs) or slowly adapting mechanoreceptors
355 (SAMs), CVs < 10 m/s as A_δ fibers, and CVs < 1.5 ms/ as C-fibers.

356 Mechanically sensitive units were stimulated using a piezo actuator (Physik Instrumente (PI) GmbH & Co.
357 KG, model P-841.60) connected to a force sensor with a calibrated conversion factor of Volts to
358 Millinewtons. Various mechanical stimulation protocols were employed to identify and characterize
359 sensory afferents. Vibrating stimuli with increasing amplitude and 20Hz frequency were applied to all
360 types of mechanoreceptors, and the force required to evoke the first action potential was measured. A ramp
361 and hold step with constant force (100 mN) was repeated with varying probe movement velocities (0.075,
362 0.15, 0.45, 1.5, and 15 mm s⁻¹), and only firing activity during the dynamic phase was analyzed. SAM
363 mechanoreceptors, A_δ mechanoreceptors, and nociceptors were mechanically tested with a constant ramp
364 (1.5–2 mN m/s) and hold (10 seconds of static phase) stimulation, analyzing spikes evoked during the static
365 phase. For electric search experiments, data were collected from 5 *Tenm4*^{fl/fl} (control) and 7 *Tenm4*^{CKO} mice
366 and from 4 WT (control) and 5 *Tenm4*^{KI/+} mice. For the stimulus-response-function recordings, data were
367 collected from 4 WT and *Tenm4*^{KI/+} mice and 6 *Tenm4*^{fl/fl} and 9 *Tenm4*^{CKO} mice.

368 For the PreScission application, the five types of receptors are categorized into two main groups:
369 mechanoreceptors (RA, SA, and D hairs) and nociceptors (AM and C fibers). Mechanoreceptors are
370 subjected to a 20Hz step of increasing vibration amplitude applied at 30-second intervals, while nociceptors
371 undergo a 150mM suprathreshold displacement at 30-second intervals. This protocol commences after
372 isolating a receptive field with a metal ring. Prior to stimulation, it is crucial to verify the sealing status of

373 the ring. The protocol involves stimulation for 3 minutes before applying the PreScission protease solution
374 (concentration 20% (v/v) diluted in SIF). Stimulation is continued for an additional 45 minutes. At the end
375 of the protocol, the conduction velocity is measured again to confirm the receptor's continued functionality.
376 Experiments were conducted in a blinded manner (R.G. or M.A.K. were aware of the group allocations).
377 To test for toxic (indirect) effects of cleavage products generated by the PreScission enzyme, single-unit
378 recordings were performed on wild-type mechanoreceptors with receptive fields isolated using a metal
379 ring. Simultaneously, skin from PreScission knock-in mice was treated with PreScission protease, and the
380 resulting supernatant, containing cleavage products, was applied to the receptive fields of wild-type
381 afferents. The responses of wild-type mechanoreceptors to repeated mechanical stimulation were
382 monitored for up to 45 minutes.

383

384 **Electron microscopy**

385 Saphenous nerves were dissected from four 12-week-old *Tenm4*^{CKO} and WT mice. The freshly isolated
386 nerves were fixed in 4% paraformaldehyde/2.5% glutaraldehyde in 0.1 M phosphate buffer for 48 hours at
387 4°C. Following treatment with 1% OsO₄ for 2 hours, each nerve underwent dehydration in a graded ethanol
388 series and propylene oxide before being embedded in polyresin. Nerves were sectioned using a microtome
389 into semi-thin (1 μm) and ultrathin sections (70 nm). Semi-thin sections were stained with toluidine blue,
390 and ultrathin sections were contrasted with uranyl acetate and lead acetate. Examination of semi-thin
391 sections under a light microscope was performed to determine the total number of myelinated axons within
392 the nerve. Ultrathin sections were examined using a Zeiss 910 electron microscope, and images were
393 captured at an original magnification of 2500×. The A and C fiber dimensions were analyzed⁶ using iTEM
394 software.

395

396 **Behavior**

397 Von Frey filament testing was conducted to assess touch sensitivity in the mice. Animals were acclimated
398 to the testing environment for two days in the week prior to the experiment. Paw withdrawal thresholds
399 were then assessed using a standard Semmes-Weinstein set of von Frey filaments (ranging from 0.07 to 4
400 g, Aesthesio) in accordance with the up-and-down method.¹³ The 50% paw withdrawal threshold was
401 determined using the open source software, Up-Down Reader
402 (https://bioapps.shinyapps.io/von_frey_app/).¹⁴ For the ascending dose-response experiments, von Frey
403 filament testing involved assessing each filament five times and calculating the responses as proportions.
404 The cotton swab test measured sensitivity to gentle touch (0.7 – 1.6 mN), while brush testing evaluated
405 dynamic mechanical sensitivity and measured intermediate touch sensation (>4 mN). A cotton swab
406 (puffed out to approximately three times its original volume) and a soft brush (number 0) were applied to
407 the plantar surface of the hind paw with gentle strokes. Each hind paw underwent testing three times, with

408 a minimum interval of 5 minutes between consecutive tests. The number of withdrawals throughout the
409 trials was counted and coded as a percentage of the total trials.

410 For Hargreaves assay, mice were acclimated for 30 minutes before the test. The infrared light source (Ugo
411 Basile, 37370) was applied to the hind paw plantar surface, and withdrawal latency was automatically
412 recorded. The focused radiant heat induced withdrawal within 10-15 seconds, with a 20-second cutoff to
413 prevent tissue damage. The time required to withdraw the paws were recorded as indicators of their ability
414 to assess temperature.

415 Sample sizes, described in each figure legend, were determined using GPower 3.1 software based on
416 previous studies. No animals were excluded from the analysis. The mice were aged between 8 and 15 weeks
417 old and were randomly assigned to various experimental groups, including control and other groups,
418 ensuring a balanced representation across conditions. The experimenter was blinded to the group
419 assignments during the von Frey filament testing.

420 Clasping behavior was assessed by suspending mice by the tail for 10 seconds and observing hindlimb
421 posture. Normal behavior was defined as full hindlimb extension, while clasping was identified as
422 hindlimbs retracting towards the body. Representative images were captured to illustrate hindlimb
423 extension in control mice and hindlimb clasping in *Tenm4*^{CKO} mice. Observations were scored, and the
424 incidence of clasping behavior was analyzed for statistical significance.

425 The integrity of balance and coordination was assessed using the Rotar-rod system (83x91x61 - SD.
426 Instruments, San Diego). This test is utilized to measure motor coordination and balance in mice. Mice
427 were subjected to three trials, with 5-minute inter-trial intervals. Rotarod acceleration was set to 20 rpm
428 over 240 seconds. The latency to fall (in seconds) was recorded, and the average of the three trials was
429 calculated as an index of motor coordination and balance.

430

431 **Tripartite split-GFP complementation assay**

432 The tripartite split-GFP complementation assay¹⁵ was performed in HEK293T cells (ACC 635, DSMZ)
433 cultured in DMEM (DMEM 41966) supplemented with 10% FCS and 1% Penicillin/Streptomycin. When
434 HEK293T cells reached approximately 70% confluence, they were co-transfected with GFP1-9::iRFP702
435 (Addgene #130125), mouseTenms(N-terminus)GFP10::mCHERRY, and mouseElkin1-GFP11::eBP2
436 plasmids using Fugene HD, following the manufacturer's instructions (Promega). Seven hours post-
437 transfection, the culture medium was replaced with fresh medium. After 40 hours post-transfection, cells
438 were fixed in 4% PFA, and images (eGFP, mCherry, and eBFP2) were acquired using cytationC10 (Biotek)
439 with a 20x objective. Gen5 (Biotek) was used to analyze eGFP (interaction signal), mCherry (transfection
440 signal of bait), and eBFP (transfection signal of prey) percentages of cells and fluorescence intensity. All
441 signal intensities were normalized against background before color threshold overlapping for eGFP-
442 positive (eGFP/mCherry) cell quantification.

443

444 **Cellular co-localization assay**

445 Transiently transfected N2a cells were imaged using an Airyscan fluorescence microscope (Axio, Zeiss)
446 equipped with a $\times 63$ 1.4 NA oil lens. For cells transfected with either pRP TENM4-ALFA, pRK8 mScarlet-
447 ELKIN1-EGFP, or mScarlet-PIEZO2, cells were prepared as previously described. After 48 hours of
448 transfection, cells were fixed and stained with FluoTag®-X2 anti-ALFA, as described earlier. Cells were
449 imaged in a total of four to five individual images under three experimental replicates. For each individual
450 image, cells expressing both plasmids at similar expression levels were chosen and counted based on ALFA
451 tag staining and mScarlet signals. The signal intensity in each group was normalized against control cells
452 carrying only a single signal. The occurrence of normalized signals was statistically analyzed using
453 Manders' Overlap Coefficient (MOC) as a colocalized indication built into ZEN.

454

455 **In vitro ALFA pull-down**

456 HEK293T cells were transfected with either Full-length C-terminally ALFA-tagged TENM4 coupled with
457 ELKIN1 or ALFA plasmid coupled with ELKIN1. Membrane protein complexes were solubilized from
458 total lysates prepared from RIPA buffer (50 mM Tris, pH 7.5, 150 mM NaCl, 1.0% NP-40, 0.5%
459 deoxycholate, 0.1% SDS, 3 mM DTT) with 1% DDM for 1 hour on ice. Both lysates were incubated with
460 20 μ L of ALFA SelectorPE resin for 1 hour at 4 °C on a roller drum. After washing in PBS containing 0.3%
461 DDM, bound proteins were eluted under native conditions by sequentially incubating twice with 50 μ L PBS
462 containing 200 μ M ALFA peptide for 30 minutes at 4°C. Samples corresponding to 1/500 of the input and
463 1/50 of eluate fractions were resolved by SDS-PAGE. Analysis was performed by Western blotting using
464 a polyclonal rabbit-raised antibody against ELKIN1 or RFP and a polyclonal sheep-raised antibody against
465 TENM4 (dilution 1:500), followed by HRPconjugated goat anti-rabbit and anti-sheep IgG (Abcam Lot:
466 GR288027-2, R&D Lot: 1522051, dilution 1:10,000). Blots were developed using the SuperSignal™ West
467 Dura ECL Kit (Thermo Scientific) and imaged using a Bio-Rad ChemiDoc™ MP imaging system. Affinity
468 purification of PIEZO2-mScarlet and TENM4-ALFA are performed as above.

469

470 **Microscopy setups**

471 Epifluorescence images were obtained with an LSM880 Airyscan microscope (Carl Zeiss GmbH),
472 equipped with a $63\times$ NA1.4 oil immersion lens, and operated the Airyscan detector in super-resolution
473 mode. This results in a pixel size of 35 nm. Excitation laser lines are 488, 561, and 680 nm. Independent
474 tracks are used to switch between lines with a Z-stack according to the sample thickness in 0.2 μ m
475 spacemen. Each line of the image is first scanned at 488 nm or 561 nm and subsequently at 561 nm. Pixel
476 dwell times are adjusted to a value between 1 and 2 microseconds with fourfold line averaging. After
477 acquisition, Airyscan processing with default (=auto) parameters is employed, which results in a 16-bit

478 image. This is stored in the proprietary CZI file format. data processing and signal quantification were
479 performed using ImageJ.

480

481 **Mass spectrometry analysis**

482 The cell lines analysed were control Neuro2a cells or Neuro2a cells with a *Piezo1* genomic deletion as
483 described previously ⁷. The samples were lysed using 1% (w/v) sodium dodecyl sulphate and 1% (v/v)
484 NP40, followed by SP3-bead-based digestion in an automated process utilising the AssayMAP Bravo
485 robotic system (Agilent Technologies; adapted from).¹⁶ In brief, protein lysates were treated with 5 mM
486 dithiothreitol (DTT; Sigma-Aldrich) and heated to 90°C for 10 minutes for reduction. Alkylation was
487 performed at room temperature with 10 mM iodoacetamide for 30 minutes, followed by quenching with
488 20 mM DTT for an additional 3 minutes. A mixture of 1 mg paramagnetic beads, comprising Sera-Mag
489 Speed Beads, CAT# 09-981-121, and CAT# 09-981-123 (Thermo Fisher Scientific), was added, along with
490 acetonitrile to a final concentration of 70% (v/v), and incubated for 18 minutes at room temperature. Beads
491 were washed thrice with 200 µl 70% (v/v) ethanol, with 3-minute incubation at each step. Subsequently,
492 150 µl HEPES-KOH (pH 7.6) was added, followed by 4 µg of sequencing-grade LysC (Wako) and trypsin
493 (Promega) for overnight incubation at 37°C. The supernatant was acidified with formic acid, and peptide
494 solution was desalted using the AssayMap protocol. For reversed-phase liquid chromatography coupled to
495 mass spectrometry (LC-MS) analysis, 1 µg of peptides per sample replicate was injected into an EASY-
496 nLC 1200 system (Thermo Fisher Scientific) for separation employing a 110-minute gradient. Mass
497 spectrometric measurements were conducted using an Exploris 480 (Thermo Fisher Scientific) instrument
498 operating in data-independent acquisition (DIA) mode. Raw files were analysed using DIA-NN version
499 1.8.1,¹⁷ in library-free mode, with an FDR cutoff 1195 of 0.01 and relaxed protein inference criteria whilst
500 using the match-between runs option. Spectra were matched against a Uniprot mouse database (2022-03),
501 including isoforms and a common contaminants database. Subsequent downstream analysis was performed
502 using R version 4.3.2. MaxLFQ normalised protein intensities were log2 transformed and filtered to retain
503 at least 4 valid values in at least one group for each protein before applying a downshift-imputation
504 procedure. Significance determination utilised the limma package,¹⁸ to compute two-sample moderated t
505 statistics, with nominal P-values adjusted using the Benjamini-Hochberg method.

506 Quantitative analysis of distinct peptides was conducted by utilising the report.tsv output generated by
507 DIA-NN, followed by application of filtering criteria wherein peptides with Protein.Q.Value and
508 Lib.Q.Value both less than or equal to 0.01 were retained for further analysis. Subsequently, the sum of
509 the three most abundant fragments was computed for each precursor. The precursor with the highest
510 abundance (Top1) was then selected for each distinct peptide sequence to facilitate peptide-level
511 quantitation. Peptide maps were constructed by calculating position-based intensities, obtained by dividing
512 the intensity of each peptide sequence by its respective length. In cases where multiple sequences of the

513 same stretch were identified, intensities were aggregated to account for miscleavages or overlapping
514 peptide sequences. Peptide intensities are not normalised. The mass spectrometry proteomics data have
515 been deposited to the ProteomeXchange Consortium via the PRIDE partner repository with the dataset
516 identifier PXD050952.¹⁹

517

518 **Immunogold labeling and transmission electron microscopy**

519 Dissociated DRG neurons were fixed by adding an equal volume of 8% Paraformaldehyde Aqueous
520 Solution (PFA, pH 7.4, pre-warmed to 37 °C) in 2x PBS to the culture medium to obtain a final
521 concentration of 4% PFA and 1x PBS. After 15 min at room temperature, the fixative was replaced with
522 fresh 4% PFA in 1x PBS, and samples were incubated for an additional hour at 4°C. Following three washes
523 in PBS, neurons were blocked in 10% normal goat serum in PBS 1x for 30 min at room temperature and
524 incubated overnight at 4 °C with the TENM4-C-terminal antibody diluted 1:200 or 1:500 in blocking
525 solution. After three PBS washes, cells were incubated for 1h at room temperature with 12 nm or 6 nm
526 Colloidal Gold AffiniPure® Goat Anti-Rabbit IgG (H+L) (1:30 dilution in blocking solution), followed by
527 three final PBS washes. Labeled samples were then prepared for subsequent resin embedding and ultrathin
528 sectioning for electron microscopy.

529 Following pre-embedding immunogold labelling, DRG neurons were fixed additionally in 4% PFA (v/v)
530 and 2.5% glutaraldehyde (v/v) in 0.05 M HEPES for 2 hours at room temperature. Samples were processed
531 using a modified version of the rOTO protocol by²⁰. Samples were contrasted with 2% (v/v) Osmium
532 Tetroxide Aqueous Solution and 1.5% (w/v) potassium ferrocyanide in 0.05 M HEPES for 60 minutes on
533 ice, washed with 0.1% (w/v) thiocarbohydrazide for 10 minutes, followed by an incubation in 1% (w/v)
534 osmium tetroxide for 30 minutes at RT. Final contrast was achieved by an incubation in 1% (w/v) uranyl
535 acetate for 30 minutes at RT. After dehydration through a graded series of ethanol, embedding was done in
536 Poly/Bed® 812 Embedding Media. Ultrathin resin sections (150 nm) of cells attached to the Lumox®
537 membrane were collected on slot grids and stained with 3% lead citrate. Imaging was performed at 200 kV
538 using the JEM 2100 Plus. Acquisition was done with the Xarosa camera and the Radius EM imaging
539 software package.

540 Images were acquired for the experimental condition (TENM4-C-terminal antibody) and the negative
541 control (no primary antibody). For the experimental condition, the total analyzed contact area was 176 µm²,
542 calculated as the measured cumulative neurite-laminin contact length multiplied by the section thickness
543 (0.15 µm); a comparable contact area (>180 µm²) was imaged for the negative control. Gold particles
544 located within 200 nm of the neurite membrane were counted and classified as being at the neurite-laminin
545 interface or elsewhere. Gold-labeled tethers were defined as electron-dense structures at the interface that
546 were associated with at least one gold particle. Tether density was calculated either relative to the total
547 contact area or to the contact area of neurites with at least one gold particle. Neurites were classified
548 according to the number of associated tethers, and tethers were further categorized based on the number of

549 associated gold particles, yielding the distributions of tethers per neurite and gold particles per tether,
550 respectively.

551

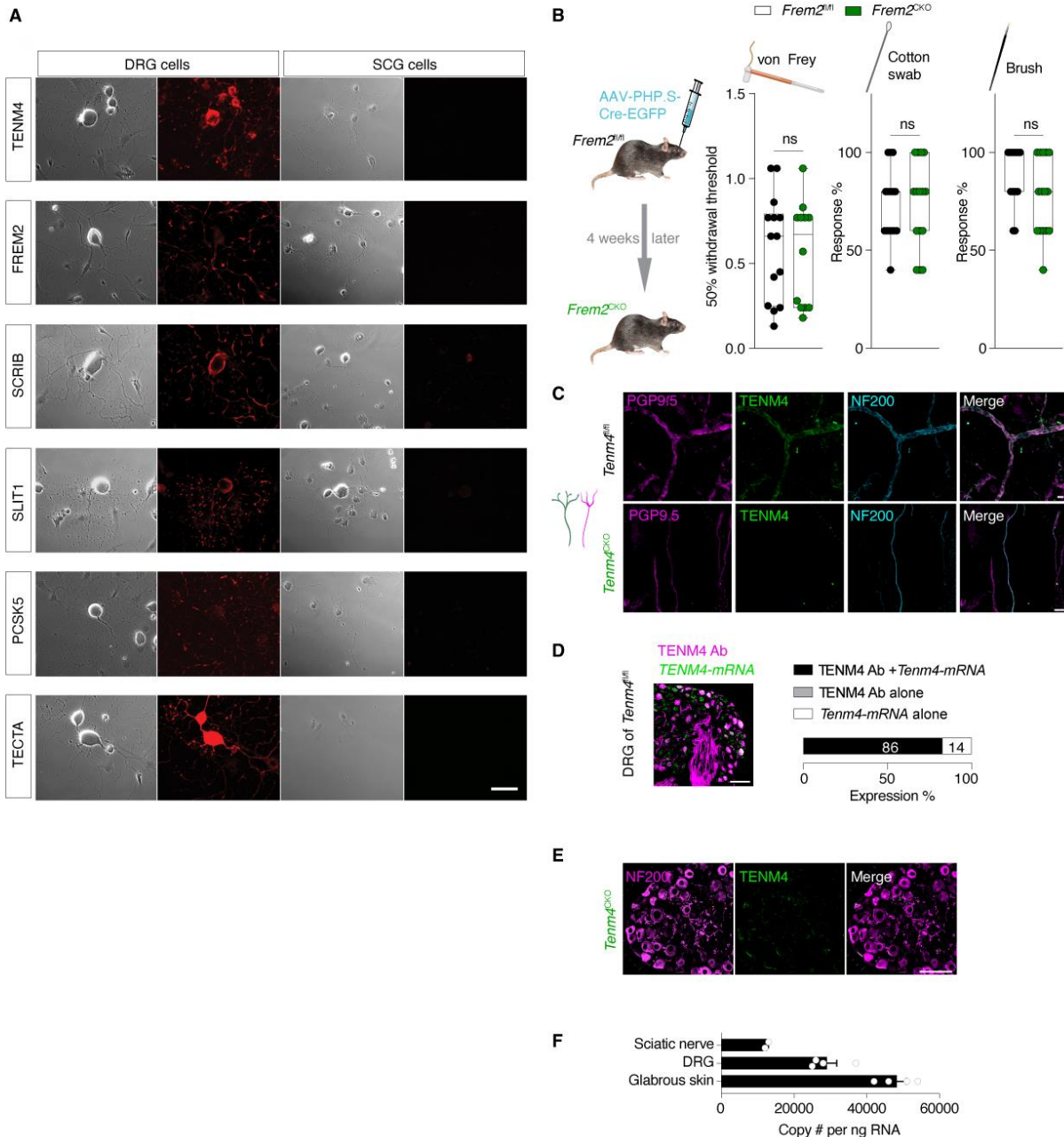
552 **Statistical analysis**

553 Statistical analyses were performed using GraphPad Prism (version X). The study employed a variety of
554 tests for different experimental assessments. Chi-squared and Fisher's exact tests evaluated proportions of
555 neuron types, Mann-Whitney tests compared various responses, and Two-way repeated measures ANOVA
556 with Sidak's post-test assessed stimuli-induced firing activity. Additionally, the impact of PreScission
557 protease treatment was scrutinized with Friedman tests, Dunn's multiple comparisons tests, and Fisher's
558 exact tests. The strength of interaction between ELKIN1 and TENM4 was determined via One-way
559 ANOVA. A comprehensive statistical strategy, including Kruskal-Wallis tests, was implemented to analyze
560 various datasets. Steps were taken to ensure that control and experimental groups were spread across
561 different days to reduce bias.

562

563

Figure S1



564

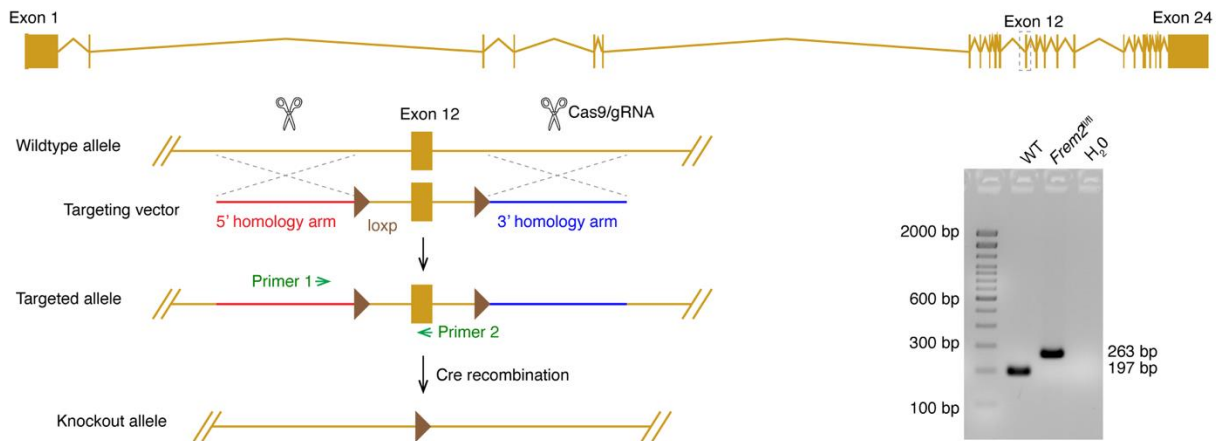
565 **Figure S1. Tether candidate screen and validation of TENM4 deletion.** (A) The 6 tether protein
 566 candidates exhibit a patchy-like expression pattern in the neurites of DRG cells, and no staining was
 567 observed in the non-mechanosensitive SCG cells cultured on plates coated with laminin. Scale bar is
 568 10 μ m. (B) Left, a diagram depicting generation of *Frem2^{CKO}* mice via retro-orbital injection of *pAAV-Syn-
 569 Cre-p2A-EGFP* in the sinus of *Frem2^{fl/fl}* mice. Right, *Frem2^{CKO}* mice exhibit normal touch sensitivity
 570 compared to the control *Frem2^{fl/fl}* mice. (C) TENM4 positive staining found in nerve endings (in hairy
 571 skin), visualized by PGP9.5 (a neuronal marker) and NF200 in WT mice (top panels). *Tenm4^{CKO}* mice
 572 exhibit a notable decrease in TENM4+ sensory nerve endings (below panels). Scale bar 20 μ m. (D) Left,
 573 representative image demonstrates the colocalization of a smFISH probe targeting *Tenm4* mRNA with the

574 TENM4 antibody staining. Right, quantification of TENM4+ sensory neurons stained with both the
575 smFISH probe and the antibody. Scale bar is 100 μ m. Quantification in each group from 2 male and 3
576 female mice; more than 700 neurons were counted in each group. (E) Representative DRG sections
577 showing absence of TENM4+ DRG cells in sections from *Tenm4*^{CKO} mice, NF200 staining was
578 unchanged, scale bar 100 μ m. (F) Quantification of *Tenm4* mRNA expression level (copies of transcript
579 per ng total RNA) in skin, DRG, and sciatic nerve. Quantification in each group from 2 male and 2 female
580 mice.

Figure S2

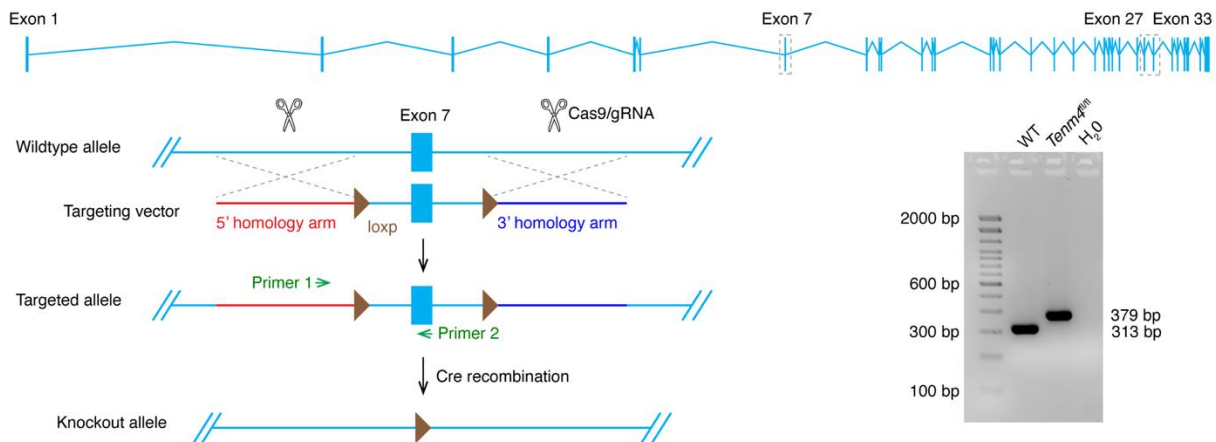
A

Frem2^{CKO}



B

Tenm4^{CKO}



C

Tenm4^{KI/+}

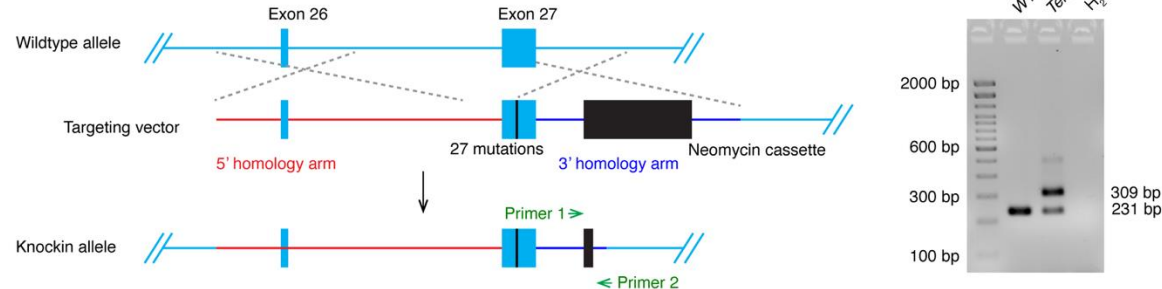


Figure S2. Strategies of generating transgenic mice. (A) Schematic of the *Frem2*^{CKO} mouse model targeting strategy using a targeting vector constructed with Infusion technology. The plasmid structure includes a 5' homologous arm (3.0kb), a LoxP sequence (1.0kb), and a 3' homologous arm (3.0kb). Right,

PCR bands from genomic DNA of WT, *Frem2*^{fl/fl} are presented. (B) Diagram depicting *Tenm4*^{CKO} mouse model creation with an Infusion-constructed targeting vector (5' homologous arm: 3.0 kb, flox: 0.9 kb, 3' homologous arm: 3.0 kb), along with PCR bands from genomic DNA of WT and *Tenm4*^{fl/fl} mice. (C) Diagram illustrating the creation of the *Tenm4*^{KI/+} mouse model using homologous recombination in ES cells. The targeting vector was designed to introduce a 21 bp change in exon 27 of Tenm4 (5' homologous arm: 7.9 kb, and 3' homologous arm: 2.5 kb) and the neomycin selection cassette, flanked by FRT sites. The neomycin cassette excision was performed by crossing the resulting chimeric mice with C57BL/6 FLP mice, leaving one FRT site (78 bp), which was used for genotyping Tenm4 KI mice. On the right, PCR bands from genomic DNA of WT and *Tenm4*^{KI/+} mice are displayed.

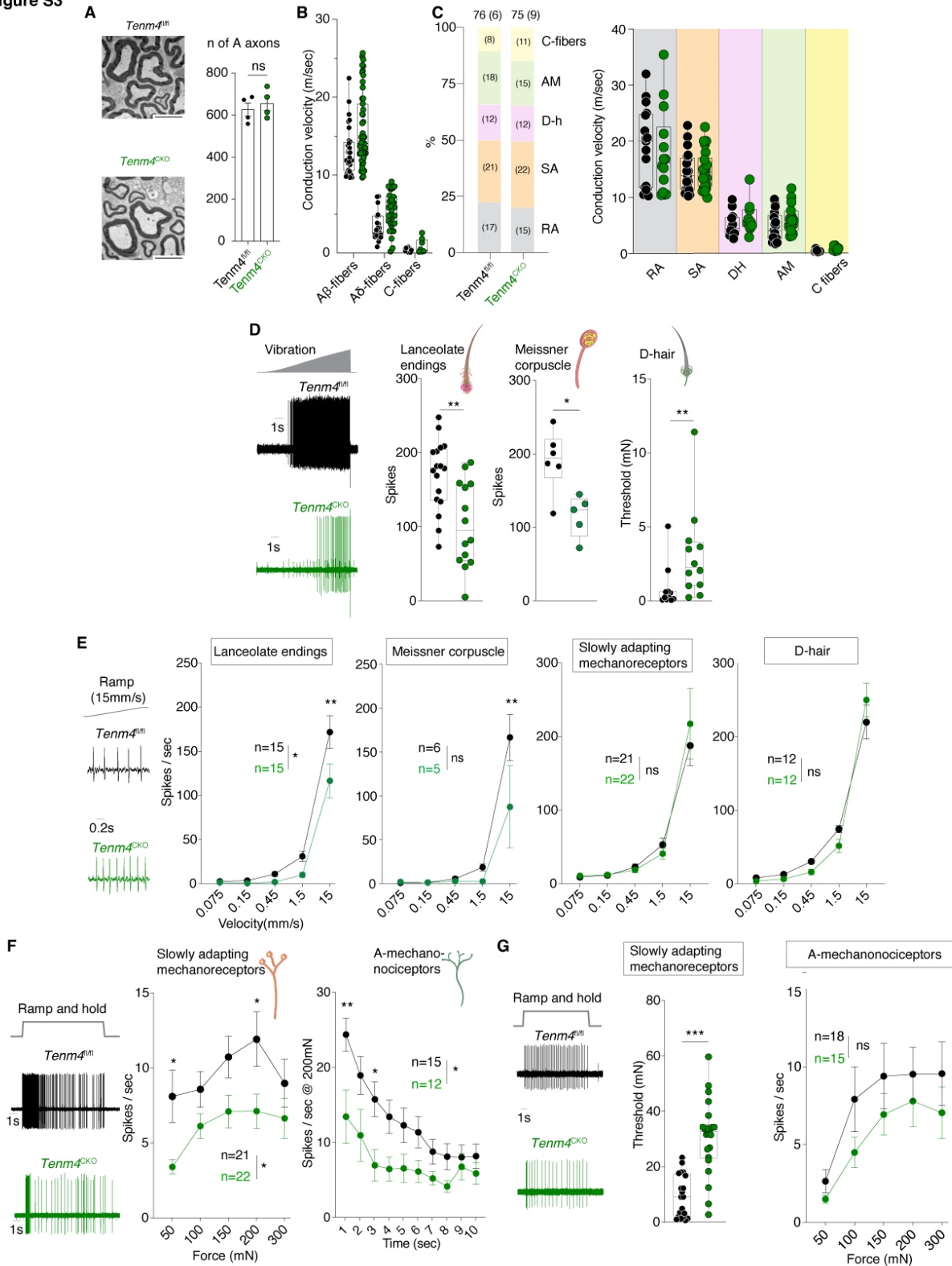
Figure S3

Figure S3. Stimulus-response functions after *Tenm4* gene deletion. (A) Example electron-micrographs from the saphenous nerve of a *Tenm4*^{fl/fl} (top) and *Tenm4*^{CKO} mouse (bottom) with quantification

of axon number in each case. Scale bar is 20 μ m. **(B)** Conduction velocities of sensory afferents recorded from 6 *Tenm4*^{fl/fl} and 9 *Tenm4*^{CKO} mice. **(C)** Proportions and conduction velocities of different sensory afferents recorded from 6 *Tenm4*^{fl/fl} and 9 *Tenm4*^{CKO} mice. **(D)** Example traces of vibration sensitive RAMs. Firing to vibration stimuli in RAMs associated with hairs or Meissner's corpuscles in *Tenm4*^{CKO} mice were significantly reduced. RAM A δ -fibers innervating D-hairs in *Tenm4*^{CKO} mice exhibited significantly higher mechanical thresholds compared to control mice. Significance calculated with Mann-Whitney test. **(E)** Example traces of single sensory units from *Tenm4*^{fl/fl} and *Tenm4*^{CKO} mice responding to a ramp stimulus with a 15 mm/sec movement velocity. The firing activity of sensory afferents innervating Merkel cells and D-hairs, in response to varying movement velocities, showed no significant differences between *Tenm4*^{fl/fl} and *Tenm4*^{CKO} mice. Two- way repeated measures ANOVA followed by Sidak's post-test; ns indicates $p > 0.05$. Data represent the mean \pm s.e.m and were collected from 6 *Tenm4*^{fl/fl} and 9 *Tenm4*^{CKO} mice. **(F)** Example SAM responses to a 50 mN amplitude ramp and hold stimulus. Stimulus response functions of SAMs were significantly impaired in *Tenm4*^{CKO} mice. Additionally, A δ -mechanonociceptors showed reduced firing during a 10s long 200 mN stimulus compared to control mice. Significance calculated with two-way repeated measures ANOVA followed by Sidak's post-hoc tests. Data collected from 6 *Tenm4*^{fl/fl} and 9 *Tenm4*^{CKO} mice. **(G)** Example traces of single sensory afferents innervating A δ mechanonociceptors in *Tenm4*^{fl/fl} and *Tenm4*^{CKO} mice responding to a ramp-and-hold stimulus with a constant force of 100mN. The mechanical threshold and firing activity of various sensory afferents showed no significant difference between *Tenm4*^{fl/fl} and *Tenm4*^{CKO} mice. Mann-Whitney test and Two-way repeated measures ANOVA followed by Sidak's post-test; ns indicates $p > 0.05$. The line graph represents the mean \pm s.e.m. and were collected from 6 *Tenm4*^{fl/fl} and 9 *Tenm4*^{CKO} mice.

Figure S4

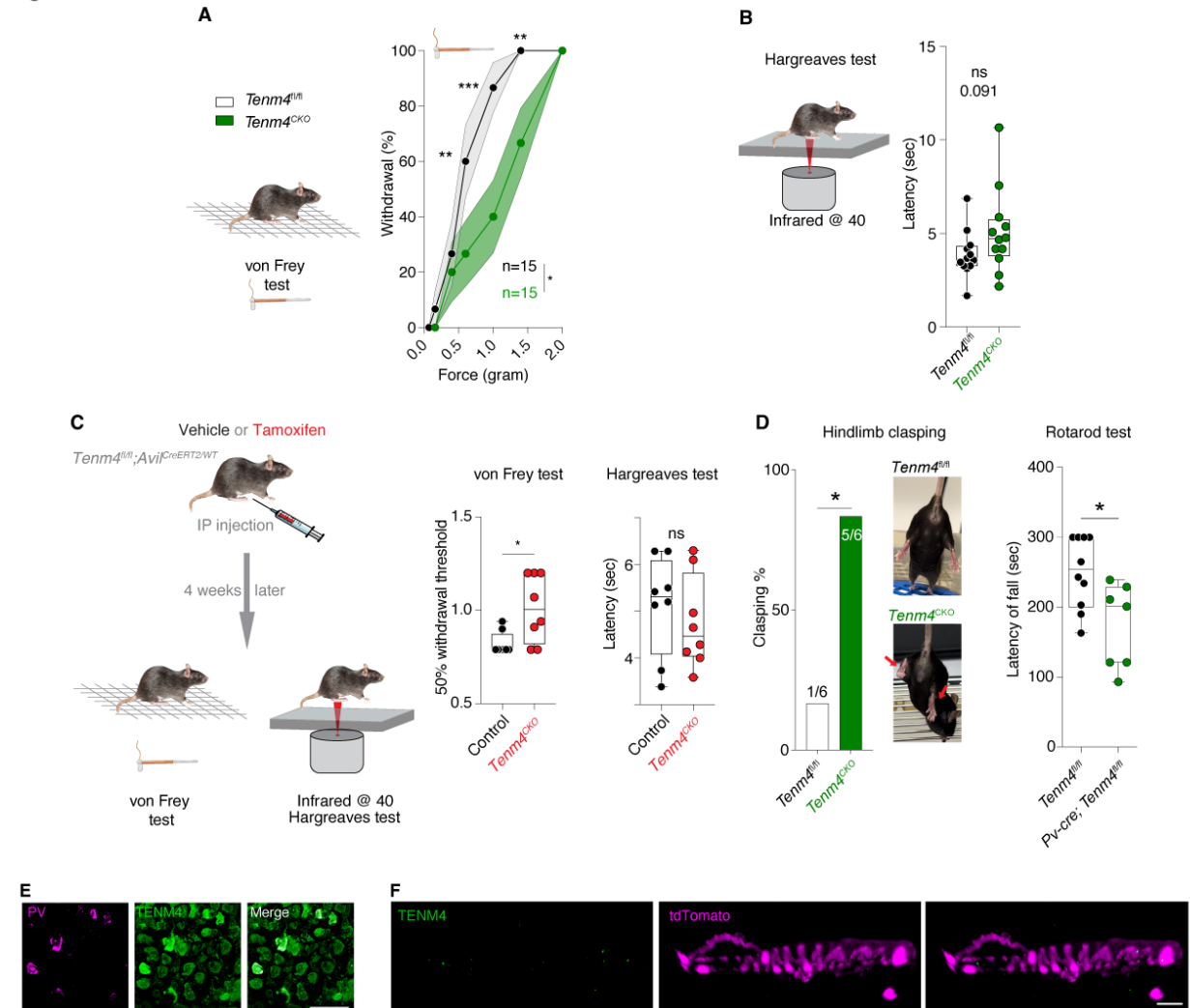


Figure S4. $Tenm4^{CKO}$ mice display mechanosensory and proprioceptive deficits but normal responses to noxious heat. (A) Responses to an ascending series of von Frey hair stimuli in $Tenm4^{CKO}$ mice. The line graph illustrates the mean represented by points and the surrounding shades indicate s.e.m. (B) Left, a Hargreaves test schematic for paw withdrawal latency, indicating thermal pain thresholds. Right, $Tenm4^{CKO}$ mice showed comparable responses to heat stimulus, similar to $Tenm4^{fl/fl}$ mice. (C) Left, a diagram illustrating the generation of $Tenm4^{CKO}$ and control mice via tamoxifen injections in $Tenm4^{fl/fl};Avil^{CreERT2/WT}$ mice. Right, $Tenm4^{CKO}$ mice exhibited significantly higher withdrawal thresholds to von Frey stimuli compared to control mice (left), while comparable responses to heat stimulus, similar to the control mice (right). Mann-Whitney test; ns indicates $p > 0.05$. Data were collected from 12 (a), 8 (b), animals per group. Means \pm s.e.m. (D) Left, A significant increase in clasping behavior is observed in $Tenm4^{CKO}$ mice, compared to controls ($Tenm4^{fl/fl}$). Representative images show normal hindlimb extension in $Tenm4^{fl/fl}$ mice (top) and hindlimb clasping in $Tenm4^{CKO}$ mice (bottom, indicated by red arrows). Right, $Pv^{Cre};Tenm4^{fl/fl}$ mice show a significant reduction in latency to fall, indicating impaired motor coordination. Each point represents an individual mouse. (E) Representative DRG sections showing double labeling of TENM4 and PV. Scale bar: 100 μ m. All PV $^+$ cells were also TENM4 $^+$. Two male and three female mice were used. (F) TENM4 expression in tdTomato-labeled muscle spindle and Golgi tendon organ afferent terminals in muscle of $PV^{Cre};Rx3^{flpo};Ai65D$ mice.

Figure S5

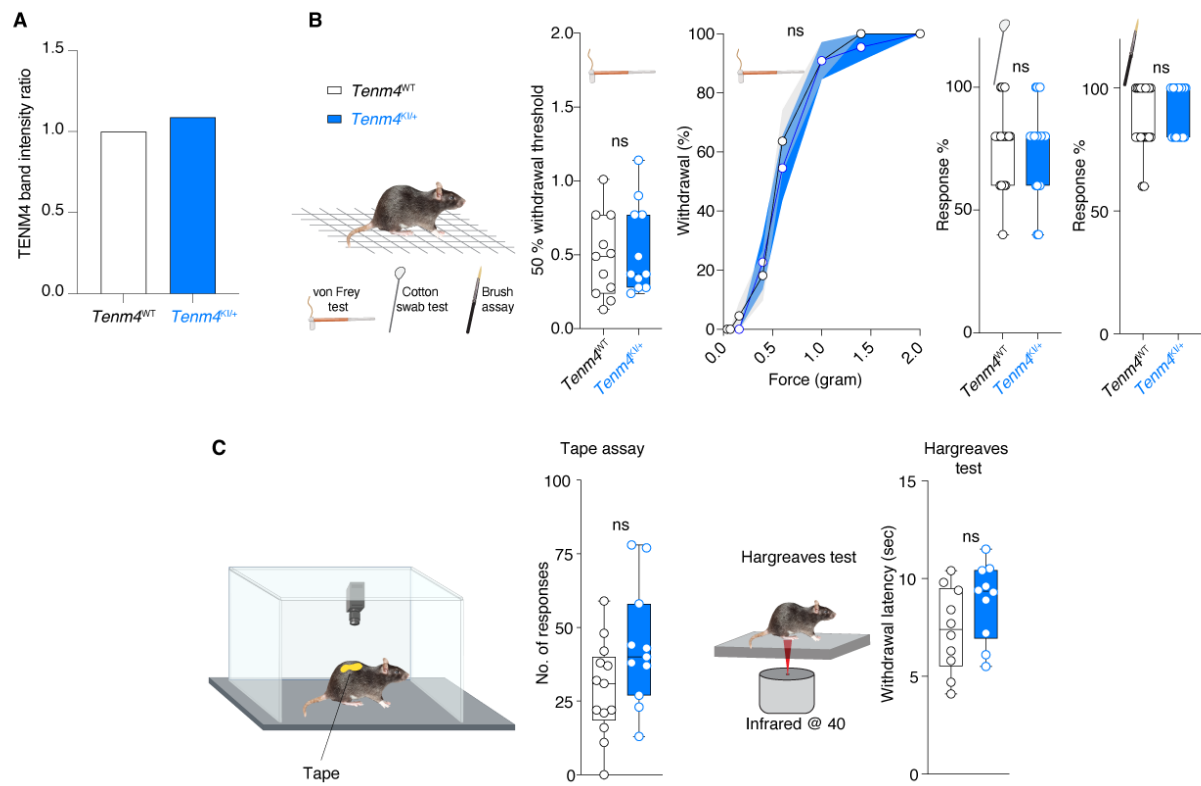


Figure S5. Behavioral characterization of *Tenm4^{Kl/+}* mice. (A) *Tenm4^{Kl/+}* mice exhibit comparable TENM4 expression to wildtype mice, indicating that the knock-in mutation does not alter overall protein abundance. (B) *Tenm4^{Kl/+}* mice exhibited similar withdrawal thresholds and responses to von Frey filaments, a cotton swab, and dynamic brush, compared to wildtype mice. (C) *Tenm4^{Kl/+}* mice display normal responses to tape and heat stimuli, similar to WT mice. Mann-Whitney test and Two-way repeated measures ANOVA followed by Sidak's post-test; ns indicates $p > 0.05$. Data were collected from 11 (von Frey, cotton swab and brush tests), 13 (tape assay) and 10 (Hargreaves test) mice in each category. The line graph represents the mean \pm s.e.m.

Figure S6

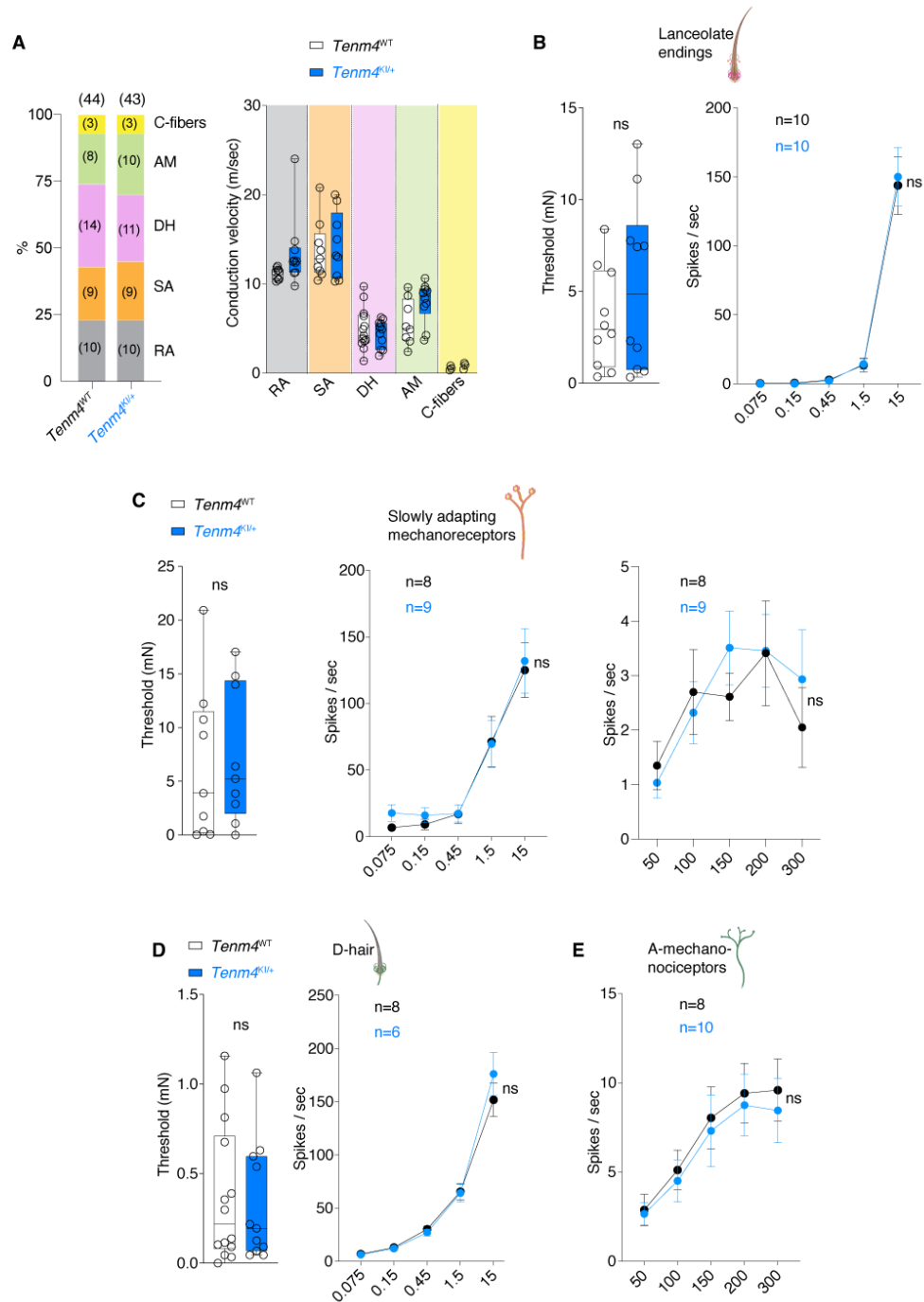


Figure S6. Electrophysiological characterization of *Tenm4*^{K1/+} mice. (A) Proportions and conduction velocities of different sensory afferents recorded from 5 WT and 4 *Tenm4*^{K1/+} mice show no marked changes. (B) The mechanical threshold and firing activity during the dynamic phase of ramp stimuli showed no significant differences between RAMs in WT and *Tenm4*^{K1/+} mice. (C) The mechanical threshold firing activity during the dynamic phase of ramp stimuli, as well as the static phase of ramp-and-hold stimuli, showed no significant differences between SAMs in WT and *Tenm4*^{K1/+} mice. (D) The

mechanical threshold and the firing activity during the dynamic phase of ramp stimuli showed no significant differences between D hairs receptors in WT and *Tenm4*^{KI/+} mice. (E) The firing activity during the static phase of ramp-and-hold stimuli, showed no significant differences between A δ mechanonociceptors in WT and *Tenm4*^{KI/+} mice. Mann-Whitney test and Two-way repeated measures ANOVA followed by Sidak's post-test; ns indicates $p > 0.05$. Data were collected from 5 WT and 4 *Tenm4*^{KI/+} mice. Means \pm s.e.m.

Figure S7

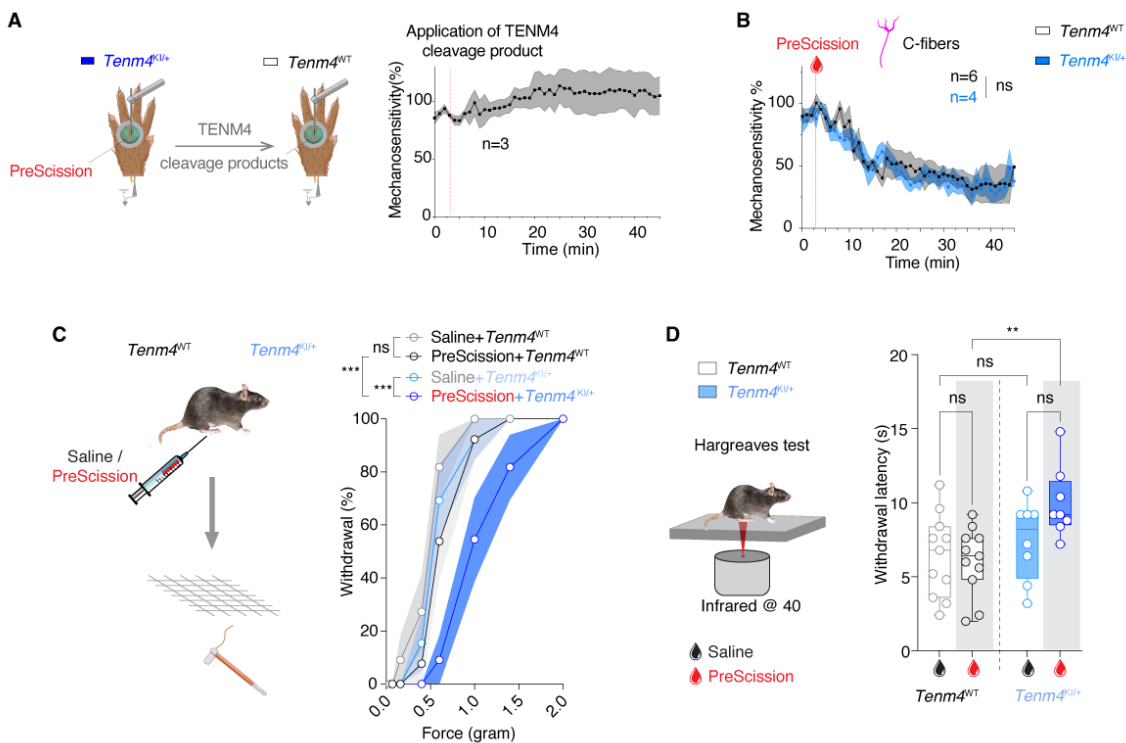


Figure S7. TENM4 cleavage impairs touch sensitivity but not C-fiber function. (A) Left, schematic showing fluid containing the cleavage product from PreScission-treated *Tenm4*^{KI/+} skin applied to the isolated receptive fields of WT mechanoreceptors. Right, mean mechanoreceptor responses (% of baseline) for RAM-A β fiber type in hairy skin, before and after the application of TENM4 cleavage product (n=3 units). Note that the mechanoreceptors retained mechanosensitivity during the 45 mins of observation. (B) C-fibers in WT and *Tenm4*^{KI/+} mice retain functionality after exposure to PreScission protease applied to their receptive fields. (C) Behavioral assays used to assess the effects of TENM4 cleavage 1 hr after PreScission injection to the plantar hind paw. The line graph illustrates the mean represented by points and the surrounding shades indicate s.e.m. A dramatic decrease in sensitivity to von Frey stimulation was observed only after treatment of *Tenm4*^{KI/+} mice with PreScission protease, and not with saline. (D) Left, Schematic of the Hargreaves test Right, *Tenm4*^{KI/+} mice injected with PreScission showed slightly longer withdrawal latencies (i.e., decreased responses) to heat stimulus, compared to PreScission-injected WT mice. Data were collected from 11 WT and 8 *Tenm4*^{KI/+} mice. Two-way repeated measures ANOVA followed by Sidak's post-test; ns indicates p > 0.05; ** indicates p < 0.01.

Figure S8

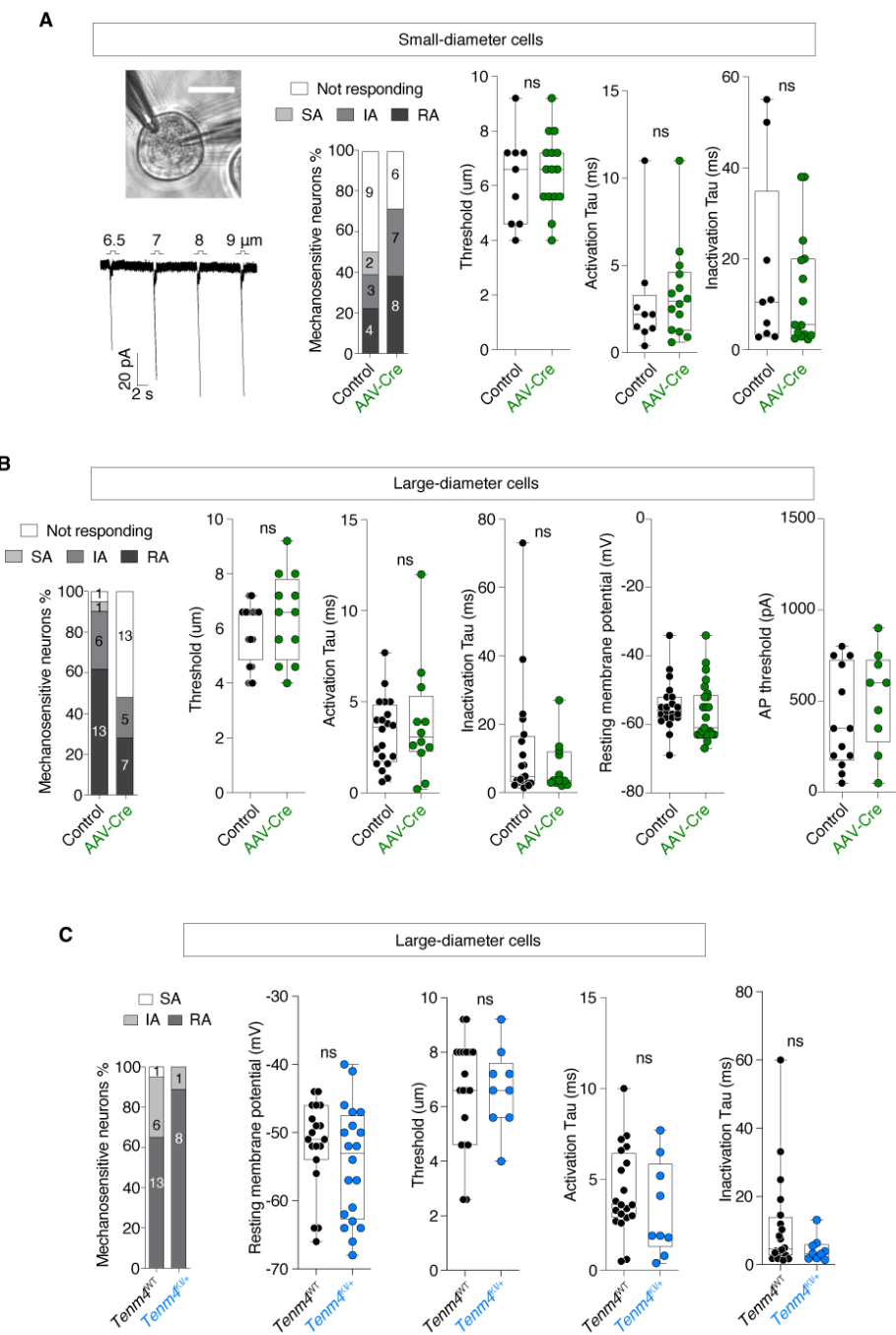


Figure S8. Mechanically activated current kinetics of DRG neurons from *Tenm4*^{CKO} and *Tenm4*^{KI/+} mice. (A) Representative traces of poking-induced currents resulting from indentations ranging between 1 and 9 μm on GFP+ large-diameter neurons in *Tenm4*^{CKO} mice. Small-diameter neurons from both *Tenm4*^{WT/WT} and *Tenm4*^{CKO} mice exhibited similar number of cells displaying rapidly, intermediate, and slowly adapting MA-currents, mechanical thresholds, as well as activation and inactivation kinetics. Chi-squared test and Mann-Whitney test; ns indicates $p > 0.05$. Data were collected from 5 *Tenm4*^{WT/WT} and 5 *Tenm4*^{CKO} mice. Means \pm s.e.m. (B) *Tenm4*^{CKO} mice had a deficit in MA-currents in large neurons compared to control *Tenm4*^{WT/WT} mice. Large-diameter neurons from both *Tenm4*^{WT/WT} and *Tenm4*^{CKO} mice exhibited similar number of cells displaying rapidly, intermediate, and slowly adapting MA-currents, mechanical thresholds, as well as activation and inactivation kinetics. Chi-squared test and Mann-Whitney test; ns indicates $p > 0.05$. Data were collected from 5 *Tenm4*^{WT/WT} and 5 *Tenm4*^{CKO} mice. Means \pm s.e.m. (C) *Tenm4*^{WT/WT} and *Tenm4*^{KI/+} mice exhibited similar number of cells displaying rapidly, intermediate, and slowly adapting MA-currents, mechanical thresholds, as well as activation and inactivation kinetics. Chi-squared test and Mann-Whitney test; ns indicates $p > 0.05$. Data were collected from 5 *Tenm4*^{WT/WT} and 5 *Tenm4*^{KI/+} mice. Means \pm s.e.m.

activation and inactivation kinetics, as well as Resting membrane potential and action potential threshold. **(C)** Recordings from large diameter sensory in culture (scale bar = 20 μ m) showed a substantial decrease in the proportion of cells with poking-induced currents, specifically in cells from *Tenm4*^{KI/+} treated with the PreScission protease. Significance calculated with Chi-squared test. Large-diameter DRG neurons from PreScission- treated WT and PreScission-treated *Tenm4*^{KI/+} mice exhibited similar percentages of rapidly, intermediate, and slowly adapting MA-currents, mechanical thresholds, as well as activation and inactivation kinetics.

Figure S9

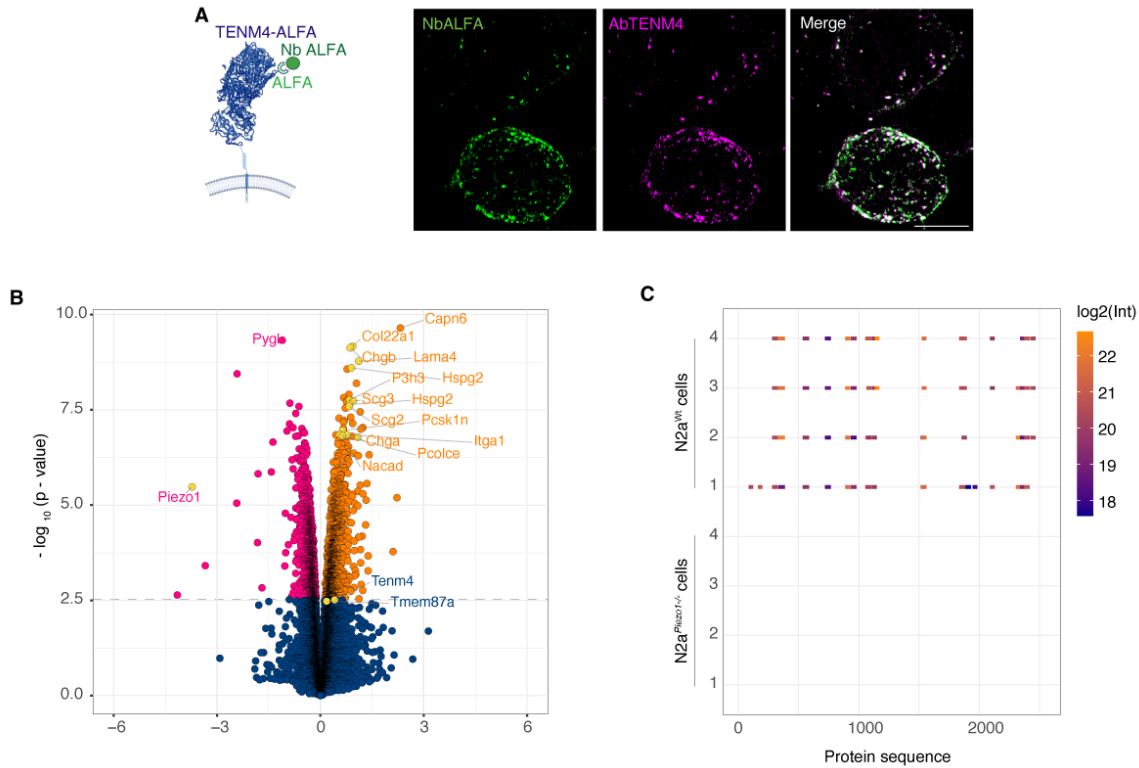


Figure S9. Generation of ALFA tagged TENM4 and the proteomic profile of N2a cells and N2a^{Piezo1-/-} cells. (A) Left, schematic of ALFA tagged TENM4. The ALFA epitope should be recognized by anti-ALFA nanobody (NbALFA) without the need to permeabilize the cells. Right, N2a cells transfected with TENM4-ALFA and stained with NbALFA labeled with AbberiorStar635P (NbALFA-Ab635P, green) and our anti-TENM4 C-terminal antibody (purple). Note the clear colocalization of the two signals (white in merge). (B) Volcano plot of mass spectrometry analyses of N2a^{Piezo1-/-} compared to WT N2a cells (n=4). Both Elkin1 (Tmem87a) and TENM4 were endogenously expressed in N2a cells and both were slightly upregulated upon Piezo1 gene deletion. Many of the proteins extensively upregulated in N2a^{Piezo1-/-} cells (highlighted in the plot) are involved either in the organization of the extracellular matrix (ECM) or in the regulation of the secretory granules, suggesting a link between mechanosensitivity and ECM composition. (C) Peptide map shows local peptide coverage of PIEZO1 in WT N2a cells. No PIEZO1 peptides were detected in the N2a^{Piezo1-/-} samples. Displayed values are in linear space whilst a log2 transformation is applied to the color scheme.

Figure S10

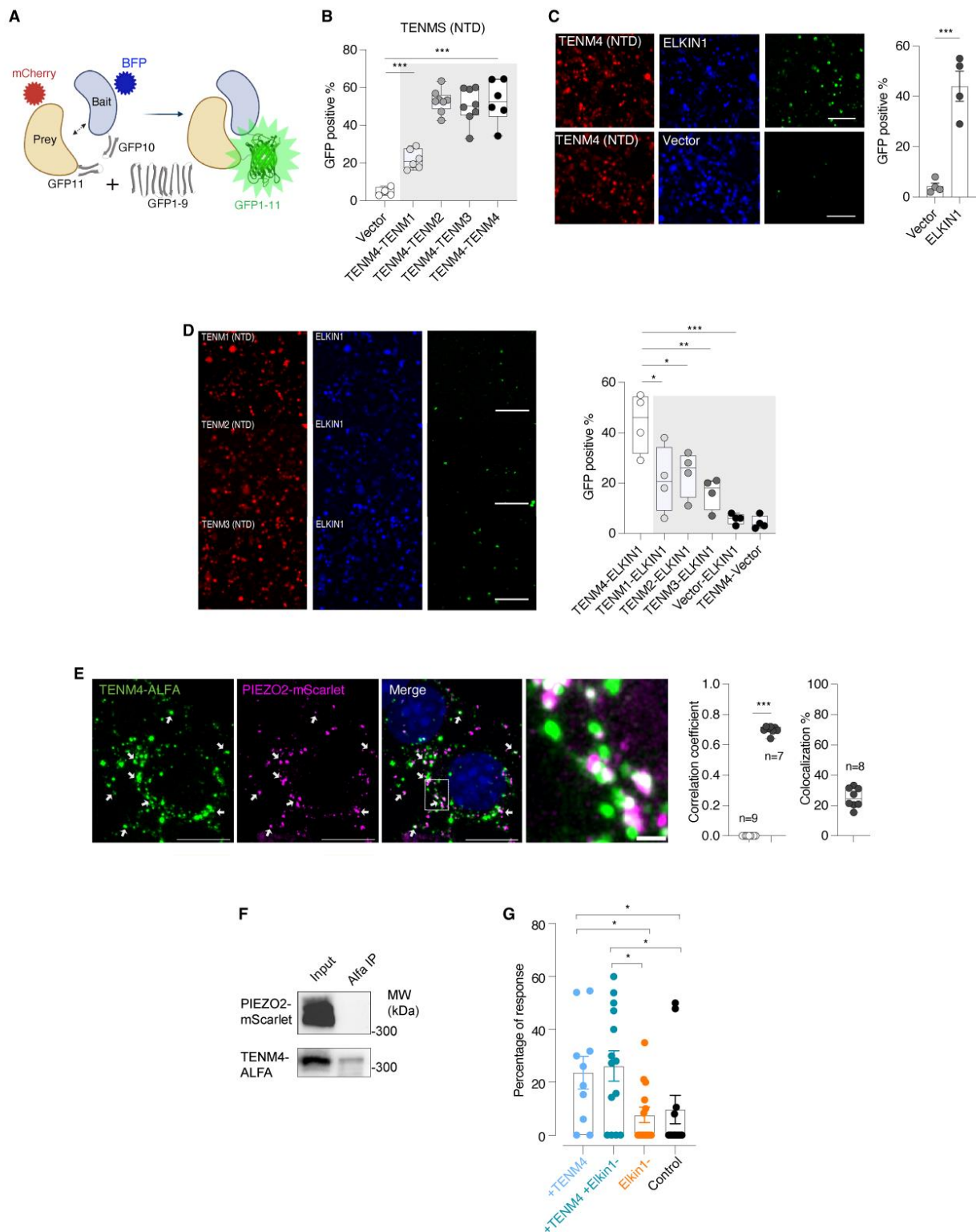


Figure S10. TENM4 interacts with other Teneurins and ELKIN1. (A) Schematic of the tripartite split-GFP complementation assay. (B) Quantification of the GFP-complementation signal in the split-GFP assay. Assay confirms heterologous interactions between the Teneurins. Pair wise interactions tested with

TENM4(NTD) between TENM1(NTD), TENM2(NTD), TENM3(NTD) and TENM4(NTD). **(C)** HEK293T cells were transfected with three plasmids encoding bait (e.g., ELKIN1)::GFP10, prey (e.g., TENM4)::GFP11 and GFP domain 1-9 proteins. Protein interaction produces complementation and reconstituted GFP fluorescence (green). Representative images showing complementation signals in cells expressing the N-terminal domain (NTD) of TENM4 showing a specific interaction with ELKIN1, not seen in the empty vector control (left 6 panels). Quantification (right) shows a strong interaction between TENM4(NTD) and ELKIN1. Scale bar 100 μ m. Statistical significance calculated with Mann-Whitney test. **(D)** Representative images depicting the tripartite-GFP interaction between ELKIN1 and other Teneurins N-terminals (TENM1 (NTD), TENM2 (NTD), or TENM3 (NTD)). Scale bar is 100 μ m. Quantification (right) shows the interaction between ELKIN1 and other Teneurins. Statistical analysis with one-way ANOVA followed by Dunnett's multiple comparison test. * indicates $p < 0.05$; ** indicates $p < 0.01$; *** indicates $p < 0.001$ means \pm s.e.m. **(E)** Representative super-resolution images of N2a cells co-transfected with a *Tenm4-ALFA* expression plasmid with PIEZO2-mScarlet (purple), arrows indicate co-localization signals. Right higher magnification of co-localized protein region (from white dash boxes) Scale bar is 10 μ m for cells, 1 μ m magnified region. Quantification was carried out and a co-localization correlation, ranging from -1 to 1, signifies the strength of overlap. Values near 1 indicate strong co-localization, near -1 indicate separation. Right, TENM4 shows 30% with PIEZO2 on the cell surface. **(F)** HEK293T cells were co-transfected with PIEZO2-mScarlet and TENM4-ALFA. Cell lysates (Input) and proteins eluted from ALFA selector resin (Alfa IP) were analyzed by Western blot using antibodies against mScarlet and ALFA. PIEZO2-mScarlet was not detected in the ALFA pull-down together with TENM4-ALFA, indicating the interaction might not be direct. Molecular weight markers are indicated (kDa). **(G)** Percentage of cells exhibiting mechanically evoked responses to pillar deflection under the indicated conditions. N2a cells were transfected with *Tenm4-ALFA*, *Elkin1* siRNA, both, or control siRNA. Dots represent individual cells from 3 mice; bars show mean \pm SEM. $p < 0.05$.

Figure S11

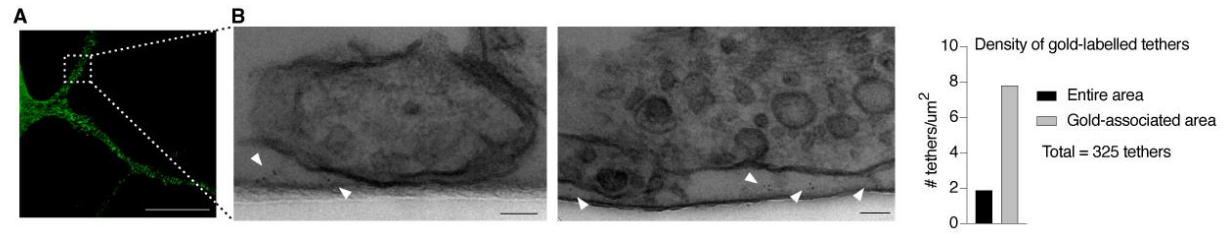


Figure S11. TENM4 is located at sensory tethers. (A) Immunofluorescence image of a mouse sensory neurite stained with the Anti-TENM4-C antibody recognizing extracellular TENM4 epitopes, showing a punctate membrane distribution of TENM4 along the neurite. Scale bar: 20 μm . (B) Left, Zoomed-out images for the TEM images in Figure 7B provide overall neurite context. Scale bars: 100 nm. Right, density of gold-labeled tethers calculated using either the total neurite-laminin contact area or only the area of neurites associated with at least one gold particle.

Table S1

Gene	DRG		SCG	
	Mean	SEM	Mean	SEM
Adamts12	N.E.D		N.E.D	
Adamts20	0.163	0.069	0.068	0.037
Apc2	0.177	0.013	0.037	0.015
C3	0.232	0.021	0.3	0.018
Celsr1	0.464	0.071	0.401	0.04
C1stn2	0.673	0.034	0.276	0.08
Coagulaion factor8	0.387	0.012	0.09	0.041
Col5a1	N.E.D		0.469	0.158
Dmbt1	N.E.D		N.E.D	
Fbn2	0.322	0.085	0.308	0.038
Frem2	0.362	0.062	N.E.D	
Igslf10	0.482	0.044	0.336	0.006
Madd	0.405	0.151	0.391	0.119
Notch3	0.602	0.072	0.309	0.023
Pcnxl3	0.595	0.217	0.439	0.022
Pcsk5	0.388	0.325	N.E.D	
Pkhd1l1	0.361	0.008	0.109	0.016
Pixnb1	0.66	0.053	0.541	0.002
RIKEN 672066o15	0.823	0.137	0.34	0.049
4931403E03Rik	0.103	0.016	0.178	0.028
5430411K18Rik	0.497	0.071	0.359	0.041
Robo1	0.414	0.069	0.378	0.102
Scrib	0.188	0.066	N.E.D	
Slit1	0.234	0.025	N.E.D	
Slit2	0.568	0.043	0.23	0.07
Stab1	0.519	0.034	0.482	0.019
Strc3	N.E.D		N.E.D	
Svep1	0.572	0.01	0.36	0.178
Tecta	0.287	0.041	N.E.D	
Tenm1	0.718	0.111	0.398	0.186
Tenm2	0.656	0.01	0.526	0.19
Tenm3	0.686	0.048	0.51	0.076
Tenm4	0.28	0.059	N.E.D	
Thsd7a	0.992	0.049	0.995	0.01

Table S1. 34 extracellular proteins with furin cleavage sites. A bioinformatics approach identified 11,302 mouse genome proteins with at least one furin cleavage site RX(K/R)R. Using DAVID, these proteins were categorized by extracellular matrix localization, sequence size, and DRG expression patterns via GenePaint ²¹, revealing 33 proteins with DRG staining signals. Following qPCR quantification of mRNA levels using HRPT as a housekeeping gene (N.E.D., no expression detected), six proteins (highlighted in yellow) were chosen as promising candidates for their specificity to DRG.

Table S2

Accession	Description	Size (aa)	DRG expression
8AQT_A	Chain A, Processed angiotensin-converting enzyme 2,Ig gamma-2A chain C region, membrane-bound form	886	No
8AQW_A	Chain A, Processed angiotensin-converting enzyme 2,Ig gamma-2A chain C region, A allele	884	No
7XMS_S	Chain S, Signle chain viable fragment of antibody	292	Not available
6NJL_K	Chain K, 15F1 Fab heavy chain	262	Not available
5ZRY_A	Chain A, Ankyrin repeat and SAM domain-containing protein 1A,Ephrin type-A receptor 6	194	Yes
6TFB_A	Chain A, Frizzled-8	138	Yes

Table S2. Extracellular proteins with a consensus PreScission cleavage site. Using a peptide search of the mouse proteome we found six proteins were detected with at least one PreScission consensus cleavage site LEVLFQ/GP.

References:

1. Hippenmeyer, S., Vrieseling, E., Sigrist, M., Portmann, T., Laengle, C., Ladle, D.R., and Arber, S. (2005). A developmental switch in the response of DRG neurons to ETS transcription factor signaling. *PLoS Biol* 3, e159. <https://doi.org/10.1371/journal.pbio.0030159>.
2. Madisen, L., Garner, A.R., Shimaoka, D., Chuong, A.S., Klapoetke, N.C., Li, L., van der Bourg, A., Niino, Y., Egolf, L., Monetti, C., et al. (2015). Transgenic mice for intersectional targeting of neural sensors and effectors with high specificity and performance. *Neuron* 85, 942–958. <https://doi.org/10.1016/j.neuron.2015.02.022>.
3. Oliver, K.M., Florez-Paz, D.M., Badea, T.C., Mentis, G.Z., Menon, V., and de Nooij, J.C. (2021). Molecular correlates of muscle spindle and Golgi tendon organ afferents. *Nat Commun* 12, 1451. <https://doi.org/10.1038/s41467-021-21880-3>.
4. Patkunarajah, A., Stear, J.H., Moroni, M., Schroeter, L., Blaszkiewicz, J., Tearle, J.L., Cox, C.D., Furst, C., Sanchez-Carranza, O., Ocana Fernandez, M.D.A., et al. (2020). TMEM87a/Elkin1, a component of a novel mechanoelectrical transduction pathway, modulates melanoma adhesion and migration. *eLife* 9. <https://doi.org/10.7554/eLife.53308>.
5. Aricescu, A.R., Lu, W., and Jones, E.Y. (2006). A time- and cost-efficient system for high-level protein production in mammalian cells. *Acta Crystallogr D Biol Crystallogr* 62, 1243–1250. <https://doi.org/10.1107/S0907444906029799>.
6. Ojeda-Alonso, J., Begay, V., Garcia-Contreras, J.A., Campos-Perez, A.F., Purfurst, B., and Lewin, G.R. (2022). Lack of evidence for participation of TMEM150C in sensory mechanotransduction. *J Gen Physiol* 154. <https://doi.org/10.1085/jgp.202213098>.
7. Moroni, M., Servin-Vences, M.R., Fleischer, R., Sánchez-Carranza, O., and Lewin, G.R. (2018). Voltage gating of mechanosensitive PIEZO channels. *Nature Communications* 9, 1096. <https://doi.org/10.1038/s41467-018-03502-7>.
8. Poole, K., Herget, R., Lapatsina, L., Ngo, H.D., and Lewin, G.R. (2014). Tuning Piezo ion channels to detect molecular-scale movements relevant for fine touch. *Nature communications* 5, 3520. <https://doi.org/10.1038/ncomms4520>.
9. Rocio Servin-Vences, M., Moroni, M., Lewin, G.R., and Poole, K. (2017). Direct measurement of TRPV4 and PIEZO1 activity reveals multiple mechanotransduction pathways in chondrocytes. *eLife* 6, e21074. <https://doi.org/10.7554/eLife.21074>.
10. Walcher, J., Ojeda-Alonso, J., Haseleu, J., Oosthuizen, M.K., Rowe, A.H., Bennett, N.C., and Lewin, G.R. (2018). Specialized mechanoreceptor systems in rodent glabrous skin. *J Physiol* 596, 4995–5016. <https://doi.org/10.1113/JP276608>.
11. Wetzel, C., Pifferi, S., Picci, C., Gök, C., Hoffmann, D., Bali, K.K., Lampe, A., Lapatsina, L., Fleischer, R., Smith, E.S., et al. (2017). Small-molecule inhibition of STOML3 oligomerization reverses pathological mechanical hypersensitivity. *Nat Neurosci* 20, 209–218. <https://doi.org/10.1038/nn.4454>.

12. Wetzel, C., Hu, J., Riethmacher, D., Benckendorff, A., Harder, L., Eilers, A., Moshourab, R., Kozlenkov, A., Labuz, D., Caspani, O., et al. (2007). A stomatin-domain protein essential for touch sensation in the mouse. *Nature* *445*, 206–209. <https://doi.org/10.1038/nature05394>.
13. Chaplan, S.R., Bach, F.W., Pogrel, J.W., Chung, J.M., and Yaksh, T.L. (1994). Quantitative assessment of tactile allodynia in the rat paw. *J Neurosci Methods* *53*, 55–63. [https://doi.org/10.1016/0165-0270\(94\)90144-9](https://doi.org/10.1016/0165-0270(94)90144-9).
14. Gonzalez-Cano, R., Boivin, B., Bullock, D., Cornelissen, L., Andrews, N., and Costigan, M. (2018). Up-Down Reader: An Open Source Program for Efficiently Processing 50% von Frey Thresholds. *Front Pharmacol* *9*, 433. <https://doi.org/10.3389/fphar.2018.00433>.
15. Cabantous, S., Nguyen, H.B., Pedelacq, J.D., Koraichi, F., Chaudhary, A., Ganguly, K., Lockard, M.A., Favre, G., Terwilliger, T.C., and Waldo, G.S. (2013). A new protein-protein interaction sensor based on tripartite split-GFP association. *Sci Rep* *3*, 2854. <https://doi.org/10.1038/srep02854>.
16. Hughes, C.S., Foehr, S., Garfield, D.A., Furlong, E.E., Steinmetz, L.M., and Krijgsveld, J. (2014). Ultrasensitive proteome analysis using paramagnetic bead technology. *Mol Syst Biol* *10*, 757. <https://doi.org/10.15252/msb.20145625>.
17. Demichev, V., Messner, C.B., Vernardis, S.I., Lilley, K.S., and Ralser, M. (2020). DIA-NN: neural networks and interference correction enable deep proteome coverage in high throughput. *Nat Methods* *17*, 41–44. <https://doi.org/10.1038/s41592-019-0638-x>.
18. Ritchie, M.E., Phipson, B., Wu, D., Hu, Y., Law, C.W., Shi, W., and Smyth, G.K. (2015). limma powers differential expression analyses for RNA-sequencing and microarray studies. *Nucleic Acids Res* *43*, e47. <https://doi.org/10.1093/nar/gkv007>.
19. Perez-Riverol, Y., Bai, J., Bandla, C., García-Seisdedos, D., Hewapathirana, S., Kamatchinathan, S., Kundu, D.J., Prakash, A., Frericks-Zipper, A., Eisenacher, M., et al. (2022). The PRIDE database resources in 2022: a hub for mass spectrometry-based proteomics evidences. *Nucleic Acids Res* *50*, D543–D552. <https://doi.org/10.1093/nar/gkab1038>.
20. Deerinck, T.J., Bushong, E.A., Ellisman, M.H., and Thor, A. (2022). Preparation of biological tissues for serial block face scanning electron microscopy (SBEM) V.2. *protocols.io*. <https://doi.org/10.17504/protocols.io.36wgq7je5vk5/v2>.
21. Visel, A., Thaller, C., and Eichele, G. (2004). GenePaint.org: an atlas of gene expression patterns in the mouse embryo. *Nucleic Acids Res* *32*, D552–6. <https://doi.org/10.1093/nar/gkh029>.